A Microfluidic Platform for Three-Dimensional Neuron Culture

Johanna Varner

S.B. Biology
Massachusetts Institute of Technology, 2006

SUBMITTED TO THE DEPARTMENT OF BIOLOGICAL ENGINEERING IN PARTIAL FULFILLMENT OF THE REQUIREMENTS FOR THE DEGREE OF

MASTER OF ENGINEERING IN BIOMEDICAL ENGINEERING
AT THE
MASSACHUSETTS INSTITUTE OF TECHNOLOGY

JUNE 2007

Signature of Author: _____
Johanna Varner
Department of Biological Engineering
June 2007

Certified by: _____
Roger D. Kamm
Professor of Mechanical Engineering and Biological Engineering, MIT
Associate Head, Department of Mechanical Engineering, MIT
Thesis Supervisor

Accepted by: _____
Bevin P. Engelward
Associate Professor of Biological Engineering
Chair, Master of Engineering in Biomedical Engineering Program

A Microfluidic Platform for Three-Dimensional Neuron Culture

by

Johanna Varner

Submitted to the Department of Biological Engineering
On May 11, 2007 in Partial Fulfillment of the Requirements for the
Degree of Master of Engineering in Biomedical Engineering

ABSTRACT

Neurodegenerative diseases typically affect a limited number of specific neuronal subtypes, and the death of these neurons causes permanent loss of a specific motor function. Efforts to restore function would require regenerating the affected cells, but progress is limited by a narrow understanding of the mechanisms that underlie the generation of these neurons from their progenitor cells. In order to prevent neuronal degeneration and potentially repair or regenerate the damaged motor output circuitry, it will be necessary to understand the molecular and genetic factors that control, direct, and enhance differentiation, axonal projection and connectivity.

While techniques are available to separate specific populations of neurons once they are fully-differentiated, current methods make it nearly impossible to monitor or control the development of a neural precursor in standard open culture. To carry out directed differentiation experiments effectively, it will be critical to control how signals are introduced to the cells. In this study, we present a microfluidic system to address the limitations of previous research. The device is capable of generating a controlled gradient of chemoattractant or growth factor of interest and directing axonal growth through an extra-cellular matrix material. Once the cells have grown into the device, signals and gradients can be applied directly to either the cell bodies or the axons. This device will serve as a platform technology for future experimentation with biomaterial scaffolds for neural tissue engineering, drug design or testing, and eventually directed differentiation of neural precursor cells.

Thesis Supervisor: Roger D. Kamm, Ph.D.
Title: Professor of Mechanical and Biological Engineering
Associate Head, Department of Mechanical Engineering

[This page intentionally left blank]

TABLE OF CONTENTS

Acknowledgements

This work would not have been possible without the help of the numerous people who have supported me throughout the year:

First, I'd like to thank my advisor, Roger Kamm. His helpful feedback at every step of the way has been invaluable to both the advancement of the project and also my understanding of the fundamental concepts behind the project. I have especially appreciated his willingness to set aside an entire day each week to meet with students and his thoughtful consideration of problems as they arose. Thank you for making this year so worthwhile.

I'd also like to thank several members of the Kamm lab who have helped me on this project. Sid Chung was been an integral part of this project before I started working on it, designing devices, doing all of the microfabrication, and training and helping me to make devices for many many experiments. Without his expertise, willingness to help, and cheerful attitude, this project would not have been possible.

Vernella Vickerman was also very helpful with useful advice about device preparation and protocols, and was immensely helpful in the FEMLAB simulations. She also patiently trained me to use several other devices not presented in this thesis.

Cherry Wan kindly fed my cells on several occasions when I couldn't come to lab. Nur Aida Abdul Rahim, Nathan Hammond and Terry Gaige also offered helpful advice, especially with my MATLAB code. All the other members of the Kamm lab have also made my time in this program both fun and educational.

This project was also performed in collaboration with Jeffrey Macklis' lab at the Harvard Stem Cell Institute at Massachusetts General Hospital, who I would also like to acknowledge. P. Hande Özdinler has been my primary contact with the Macklis lab, and she has graciously provided me with many of the mouse cortices, cell culture reagents and protocols for this project. We planned and carried out experiments together on a regular basis, and she has been very kind to share her expertise with me along the way. Akash Chandawarkar has also assisted with experiments and feeding cells that were kept at MGH. Ashley Palmer and Karen Billmers have also kindly helped dissect cortices and prepare solutions for these experiments.

All of the postnatal rat tissue came from Sebastian Seung's lab at MIT's Brain and Cognitive Science Department. Neville Sanjana, a graduate student, kindly helped

me with cell culture protocols and advice along the way. Jeannine Foley, a technician, performed dissections every week and graciously set aside several cortices for me to collect. Without their help this work would never have been possible.

Finally, I would like to thank my parents, Kathleen Digre and Michael Varner, for providing me with the means to attend MIT and for being unconditionally encouraging and supportive of my work and decisions.

This work has been funded in part by the Fidelity Foundation.

1.0 INTRODUCTION

1.1 Background

Neurons are electrically excitable cells that function to transmit and process information in the nervous system. A typical neuron consists of a soma, or cell body, a collection of branched cellular extensions called dendrites, and a long extension called the axon that can extend thousands of times the diameter of the cell body. Other cell-types in the central nervous system (CNS) include astroglia (which provide structural and metabolic support to neurons) and oligodendrocytes (which insulate CNS axons and enhance signal propagation).

The growth cone is the structure at the tip of a growing axon that is sensitive to gradients of signaling molecules. It is covered in small projections called filopodia that are in turn covered in receptors for multiple molecular cues such as attractants or repellents, diffuse signals or molecules bound to the extracellular matrix[1]. Through an undefined intracellular signaling cascade, a gradient in receptor binding is likely translated into a gradient in actin polymerization, increasing the likelihood of filopodial generation[2]. Filopodial projections can then sample the surrounding environment and exert the forces necessary to pull the growth cone and the axon forward[3].

The membrane of the cell body and the axon contain voltage-gated ion channels, proteins that control the electrical potential across the membrane and allow electrical impulses, or action potentials, to be propagated along the axon. Most neurons receive input signals at the soma and dendrites. Information is then transmitted down the axon, which connects to the soma and dendrites of target cells at a junction called the synapse. At a chemical synapse, small structures called axon terminals contain vesicles of neurotransmitter. A chemical synapse between a motor neuron and a muscle cell is called a neuromuscular junction.

1.1.1 Motor Output System Structure and Function

The motor output system is part of the central nervous system (CNS), which includes the brain and the spinal cord (Figure 1). Voluntary movements in particular are controlled by the primary motor cortex located at the precentral gyrus of the frontal lobe. The corticospinal motor neurons (CSMN) and the cortico-brain stem neurons are the

cerebral cortex component of motor output circuitry[4]. CSMN axons form the corticospinal tract, which descends through the midbrain and hindbrain to terminate on groups of motor neurons in the spinal cord or on interneurons that are associated with these motor neurons. CSMN and their associated spinal motor neurons innervate many distal muscles necessary for precise movements[5].

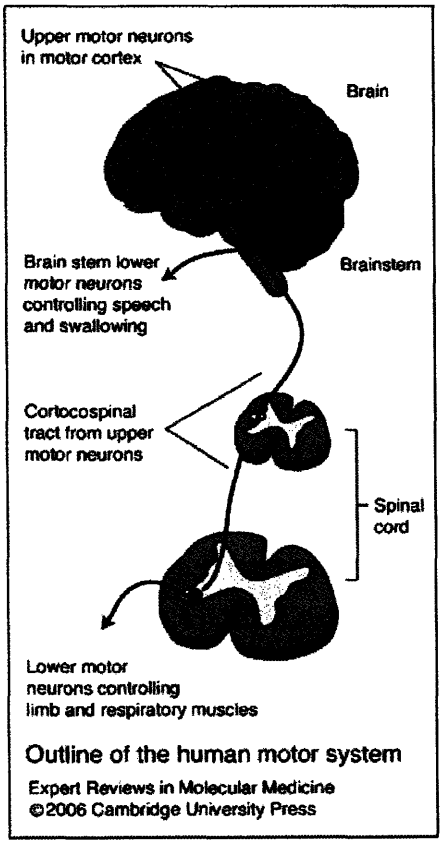

Figure 1. Outline of the human motor system. Upper motor neuron cell bodies are situated in the motor cortex and project axons via the corticospinal tracts to the spinal cord. There they synapse with lower motor neurons, which project axons that contact muscle fibers at the neuromuscular junction. Lower motor neurons originating in the brain stem or in the spinal cord may also be affected. Damage to various combinations of upper and lower motor neurons occurs in human amyotrophic lateral sclerosis. Figure from Reference [6].

1.1.2 Neurodegenerative Diseases

Neurodegenerative diseases typically affect a limited population of neurons, causing irreversible loss of a specific sensory or motor function. Amyotrophic Lateral Sclerosis (ALS, or Lou Gehrig's disease) is a neurodegenerative disorder marked by progressive dysfunction and death of the neurons in the motor pathways, resulting in generalized weakness, muscle atrophy and paralysis[7]. Respiratory failure is the most common cause of death, and generally occurs within 1-5 years of onset[8]. As many as 33,000 Americans are estimated to have the disease at any time, and more people die each year of ALS than of Huntington's disease or of Multiple Sclerosis[9]. ALS results in part from the progressive degeneration of the CSMN, which are also the targets of the

related neurodegenerative diseases hereditary spastic paraplegia (HSP) and primary lateral sclerosis (PLS)[10,11].

1.2 Stem Cell Therapy for Neurodegenerative Diseases

Many neurodegenerative diseases, like ALS, have multiple causes and cannot be diagnosed until after significant damage has already occurred, making the discovery of an effective pharmacological treatment extremely challenging. Efforts to restore function after cell death in affected individuals would require repairing or regenerating the affected cells. While there have been some promising preliminary results, progress in stem cell therapy for neurodegenerative disorders is limited by a narrow understanding of the mechanisms that underlie the generation of the affected neurons from their progenitor cells.

1.2.1 Cell Therapy and ALS

Endogenous neural stem cells that are capable of dividing into many different cell types (e.g.: neurons, astrocytes, oligodendrocytes) exist in the CNS and can be isolated and expanded in culture[12]. Transplantation experiments in rodents and primates have shown that these precursor cells or even immature neurons can survive, mature and extend axons into areas of neuronal degeneration[13]. However, ALS affects a highly specific population of neurons arranged in a complex circuit, so potential stem cell therapy for ALS will depend on whether donor cells can differentiate into necessary cell types, re-establish long-distance connections with appropriate targets, and functionally integrate into existing CNS circuitry.

In one study, fetal cortical neurons from different developmental stages were grafted into adult mouse neocortex[14]. Two weeks after the transplantation, many cells had taken on morphological features of CSMN and received afferents from the host brain. Twelve weeks after transplantation, many cells had extended projections into the contralateral hemisphere and made connections with the existing cortex. In all cases, the later-stage cells were more efficient at adopting a mature neural phenotype and making appropriate connections with existing circuitry. These results support the strategy of differentiating stem cells along a particular neuronal lineage *in vitro* and then transplanting late-stage neurons or neural precursors.

Recently it was discovered that endogenous neural precursor cells are capable of differentiating into a small number of CSMN and extending long axons into the spinal cord of adult mice[15]. A combinatorial program of transcription factors that control CSMN directed differentiation from neural precursor cells was also identified[16,17]. In addition, recent work using cultured CSMN purified by fluorescence-activated cell sorting (FACS) has defined the first peptide controls over immature CSMN development of polarity, branching of dendrites, and axon elongation. Insulin-like growth factor-1 (IGF-1) was shown to specifically enhance the extent and rate of CSMN axon outgrowth[18]. Other growth factors including BDNF, NT-3 and CNTF also enhance CSMN survival[19]. Successes with these trophic molecules suggest that directed differentiation and axonal elongation to appropriate targets could allow newly formed CSMN to connect to existing CNS circuitry.

1.2.2 Challenges to Cell Therapy

Finding an effective stem cell therapy for ALS will be particularly challenging because transplanted cells must not only differentiate into motor neurons, but also be recognized by and connect to existing CNS neurons. They must then extend axons over long distances to the appropriate location in the spinal cord or skeletal muscle. In addition, it will be important to be able to control undesired growth of stem cells, and also to protect implanted or regenerated cells from the ongoing disease process. One fundamental issue preventing effective stem cell therapy is that we do not yet have a clear picture of the molecular and genetic factors that control, direct, and enhance differentiation, axonal projection and connectivity of the affected cells.

While techniques are available to separate specific populations of neurons once they are fully-differentiated, standard open culture methods do not provide adequate control of the cell's environment, making it impossible to systematically monitor or direct the development of a neural precursor. Technological innovations will be needed to control genetic modifications or signals and how they are applied to cells. Microfluidics technology offers a potential solution to some of the problems associated with current methods.

1.3 Soft Lithography Microfabrication for Biological Studies

Microfabrication technology has been available for over 30 years in the semiconductor industry, but has only recently been applied to biology and medicine. In the past several years, microfabrication has revolutionized the fields of biology and biological engineering[20, 21]. Advantages of microfabricated systems include the ability to accurately and quickly reproduce small (μm-scale) geometries and the capacity for high-throughput experimentation. In addition, the technology is relatively inexpensive and efficient because soft lithography microfabrication does not require elaborate or expensive laboratory facilities or equipment.

This microfabrication process begins when a positive relief of the design is patterned onto a silicon wafer using photolithography methods. Once the pattern is in place, a self-curing liquid elastomer is poured onto the wafer and allowed to harden. The result is an elastomeric mold that can be used as a stamp to pattern chemicals or biological molecules onto a surface, or bonded to a glass coverslip to create a network of microfluidic channels.

Poly(dimethylsiloxane) (PDMS) is the elastomer most commonly used for biological applications. PDMS is optically transparent, easy to manipulate, and bonds tightly to glass and other PDMS surfaces after oxygen plasma treatment. This property of PDMS allows the creation of tight seals that prevent fluid leakage from a network of microfluidic channels. In addition, PDMS is nontoxic to cells[22] and gas-permeable, making it an ideal choice for cell-culture applications[23]. These microfluidic devices are perfect for biological experiments because they allow shorter reaction times, smaller sample volumes, reduced reagent requirements, and high-throughput parallel designs.

1.3.1 Microfabricated Devices Applied to Neural Cell Culture

Not surprisingly, many groups have already applied soft-lithography techniques to the study of neurons. One particularly elegant device allows axons to grow from one fluidic compartment on polylysine-coated glass surface through a series of microgrooves to another compartment[24]. A slight pressure gradient across the device allows the two compartments to remain fluidically isolated due to a small flow through the microgrooves. Depending on the pressure gradient application, a signaling molecule or chemical treatment can be localized to either the soma or the axon of a growing neuron.

Taylor et al. also used this technique to isolate mRNA from the soma and from the axons of rat cortical and hippocampal neurons, and compared gene expression in both regions of the cells.

Microfluidic systems have also been applied to stem cell differentiation. A gradient-generating microfluidic platform was used to investigate the effect of growth factor concentration on the behavior of human neural stem cells (hNSCs)[25]. hNSCs proliferate in culture, and differentiate into astrocytes in response to certain growth factors. In this device, a steady laminar-flow gradient was applied to hNSC culture and cells were able to differentiate or proliferate in direct response to growth factor concentrations. Chemical gradients have been shown to be important for both stem cell differentiation and axonal extension[26], so direct application of a gradient will be extremely useful in designing stem cell therapies for neurodegenerative disorders.

Another useful procedure made possible by microfabrication is the ability to interface electrical nanowires with living cells. Patolsky et al. recently created an array of silicon nanowire field effect transistors and directed axonal growth through the array with a pattern of adhesive molecules[27]. Each microelectrode makes an electrical interface with the axon and can be used for highly sensitive, spatially resolved detection of an action potential, or to introduce an excitatory or inhibitory signal to the cell. Using this device, the researchers were also able to carefully monitor the rate, amplitude, and shape of signals traveling along the axon or dendrites of an individual neuron.

1.4 Physiological Significance and Objective of the Present Study

There is no known cure for neurodegenerative diseases like ALS, and efforts to restore function would require regenerating the affected cells. Unfortunately, progress is limited by a narrow understanding of the mechanisms by which these neurons are generated from their progenitor cells. In order to prevent neuronal degeneration or potentially repair or regenerate the damaged motor output circuitry, it will be necessary to understand the molecular and genetic factors that control, direct, and enhance differentiation, axonal projection and connectivity. The ability to recapitulate CSMN development *in vitro* would be a first step towards functional repair of the damage caused by diseases like ALS.

While techniques are available to separate specific populations of neurons once they are fully-differentiated, current methods make it nearly impossible to monitor or control the development of a neural precursor in a precise way in standard open culture. To carry out directed differentiation experiments effectively, it will be critical to control how signals are introduced to the cells. Microfluidic platforms have proven to be very useful because the chemical microenvironment can be easily manipulated in time and space.

In this study, we present a microfluidic system to address the limitations of previous research. Cells are cultured in the device in a channel exposed to media, and axonal growth is directed through a three dimensional matrix in response to a gradient of chemoattractant or growth factor. The gel provides a natural environment for cell survival and neurite outgrowth because the cells are immersed in a three-dimensional scaffold. In previous microfluidics approaches to neural cell culture, the cells are always cultured on a two-dimensional surface and axons are patterned using adhesive molecules such as poly-L-lysine or laminin. The advantages of three-dimensional cultures have been demonstrated in numerous cell types and shown to be significant[28]. In addition, this design enables us to carefully control how signals are introduced to the cells: as a gradient in either direction, or localized to either chamber by a pressure gradient across the axon channel. We expect that this technology will be useful in future studies including: optimization of biomaterials for neural tissue engineering, examining the effects of compounds or new drugs on axon extension or neural development, and directed differentiation of neural precursor cells into highly specialized neurons.

2.0 MATERIALS AND METHODS

2.1 Neuron Isolation and Dissociation

Two sources of neural tissue were used in this study. Sebastian Seung's lab at the MIT Department of Brain and Cognitive Science kindly provided postnatal day 0 or 1 (P0-P1) Sprague-Dawley rat cortices. Rats were anesthetized on ice for five minutes, and then quickly decapitated. Brain tissue was then dissected in cold dissection solution consisting of Hank's balanced salt solution (HBSS, Life Technologies, Gaithersburg, MD) supplemented with 25 mM HEPES, pH 7.35.

The Jeffrey Macklis lab at the Massachusetts General Hospital Center for Nervous System Repair also kindly provided P0 to P2 cortices from C57BL6 mice that constitutively express GFP under a beta-actin promoter in all cells. These cortices were dissected in cold Dissociation Medium (DM) (20 mM glucose (Sigma), 0.8 mM kynurenic acid, 0.05 mM D(-)-2-amino-5-phosphonovaleric acid (AP5, Sigma), 50 U ml^{-1} penicillin (Sigma), 0.05 mg ml^{-1} streptomycin (Sigma), 0.9 M Na_2SO_4 and 0.014 M $MgCl_2$, pH 7.35). For more information on tissue sources and a comparison of the cells obtained from each source, see Appendix A.

Dissociation procedures were the same for both types of tissue. Cortices were first minced into small pieces and then washed three times in cold DM. Next, the tissue was enzymatically digested at 37°C (0.16 mg $liter^{-1}$ L-cysteine (Sigma), 12 U ml^{-1} Papain (Worthington), 0.05% DNase I (Sigma), pH 7.35, prepared in DM). After 15-20 minutes, enzymatic activity was inhibited by incubation in dissociation medium containing 10 mg ml^{-1} ovomucoid (Sigma) and 10 mg ml^{-1} bovine serum albumin (BSA). Cells were then mechanically dissociated by trituration in OptiMEM solution (OptiMEM (Gibco), supplemented with 20 mM glucose, 0.4 mM kynurenic acid and 0.025 mM AP5) and spun for 3-5 minutes at 1000 rpm to remove cellular debris. The pellet was resuspended in cold serum-containing medium (SCM; 1 mM L-glutamine (Gibco), 35 mM glucose, 37.5 mM NaCl, 10% FBS, 0.5% B27 prepared in Neurobasal A (Gibco)). Cells were then counted with a hemacytometer and plated immediately on poly-L-lysine (PLL, Sigma) coated culture plates, in collagen suspension, or in PDMS devices. For a more complete description of dissociation buffers and protocols, see Appendix B.

2.2 Neuron Culture Methods

Cortical neurons were cultured in Serum-Containing Medium (SCM) at 37°C in a humidified tissue culture incubator in the presence of 5% CO_2 for up to 7 days in vitro (DIV)). In some cases, conditioned medium was used (CM; SCM conditioned overnight on P2 cortical cells).

In order to coat surfaces with PLL, culture plates or glass cover-slips were incubated with poly-L-lysine solution (10 μg ml^{-1}, Sigma) at 37°C overnight. The plates were then washed three times with ddH_2O and allowed to dry in a laminar flow hood before cells were added (~10^6 cells ml^{-1}).

Collagen (Rat Tail Type I; BD Biosciences, San Jose, CA) was purchased in 0.02 N acetic acid and diluted in CM. Sodium hydroxide (NaOH) was added to bring the solution to pH 7.35. A small volume of cells in SCM was then added to the gel solution, bringing it to a final collagen concentration of 0.35 to 2.0 mg/ml, and cells were plated immediately in culture dishes or in PDMS devices. The gel was allowed to set by incubation in a humidified tissue culture incubator at 37°C for 10-20 minutes.

2.3 Microfabrication of Experimental System

2.3.1 Design of Experimental System

Our microfluidic system was designed and fabricated with the ultimate goal of directing axon outgrowth through a three-dimensional matrix in response to a chemical gradient. A brief schematic is shown below in Figure 2. All designs were drawn in AutoCAD (Autodesk, Inc. San Rafael, CA).

2.3.2 Patterning the Channel Design onto a Silicon Wafer

The design was first printed onto a transparency mask. The design was then patterned onto the silicon wafer using a microfabrication process called two-level photolithography (Figure 3). A complete protocol for two-level photolithography can be found in Appendix C. The silicon wafer (Wafemet, Inc., San Jose, CA) was first dehydrated for 10 minutes at 200°C. A thin layer of SU-8 2050 photoresist (Microchem Corp., Newton, MA) was then spin-coated into a thin layer on the wafer. This first layer was the desired height of the axon channel. The coated wafer is then soft baked, and

step-exposed to UV-light five times through the first transparency, which patterns the axon channel and gel-filling channel. The areas exposed to UV light through the transparency become cross-linked when the wafer is post exposure baked.

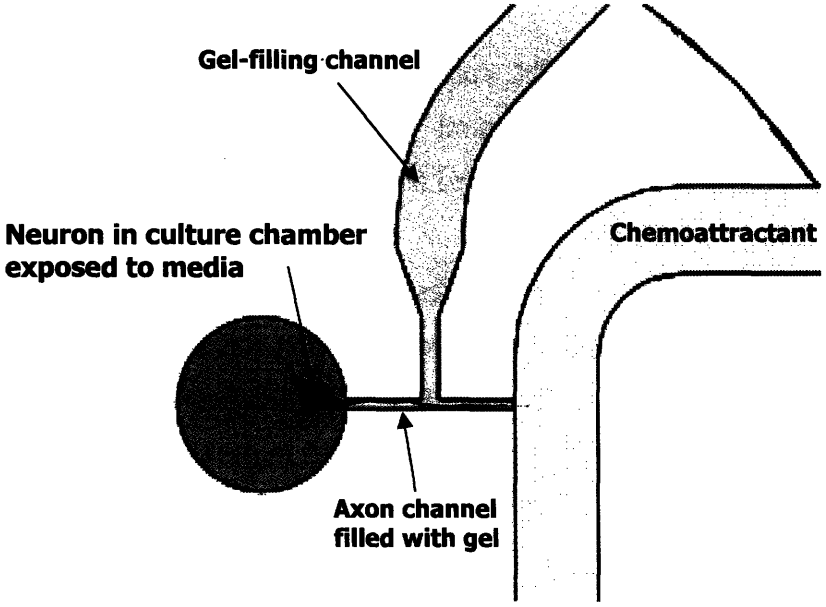

Figure 2. Device Design Schematic. The gel-filling channel is first used to introduce liquid ECM components into the axon channel, which connects the cell chamber to the chemoattractant channel. Cells are then cultured in a cell culture chamber exposed to media, and neurites are directed into the adjoining axon channel. In the absence of flow, a stable diffusive gradient of chemoattractant will be present in the axon channel. (Image adapted from S. Chung)

In order to pattern the chemoattractant channel and the cell culture chamber, the same wafer was next spin-coated with SU-8 2050 photoresist to a thickness of approximately 120 μm, and soft baked. The second transparency mask was aligned over the pattern of axon and gel-filling channels using an alignment grid found on both masks. The wafer was then step-exposed to UV light again, and post exposure baked to crosslink the exposed regions. Finally, an SU-8 developer (Microchem Corp., Newton, MA) was washed over the wafer to develop the channel features, and the wafer was rinsed with isopropyl alcohol and dried with pressurized, filtered nitrogen.

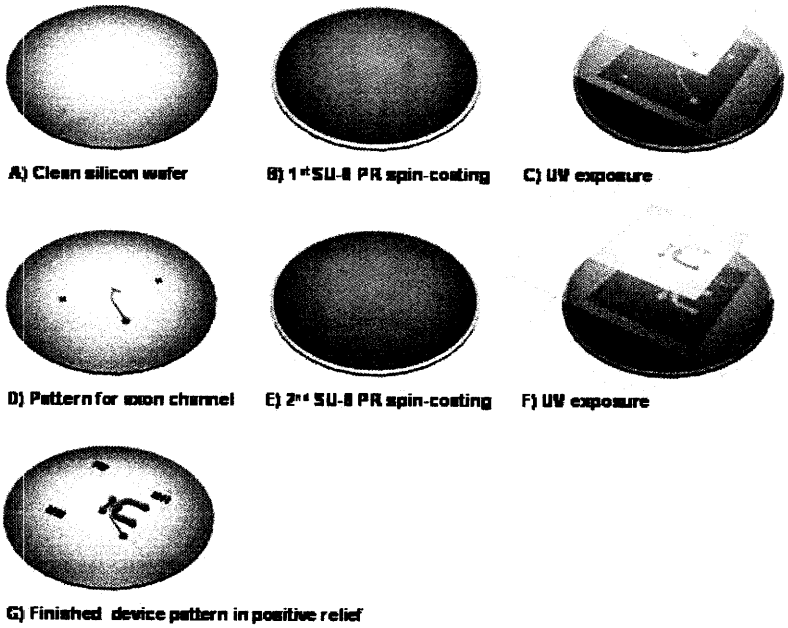

Figure 3. Two-Level Photolithography. The finished microfluidic channel pattern (G) is created in two sequential stages of SU-8 photoresist coating (B,E) followed by exposure to UV light (C, F) through a transparency mask. (Image courtesy of S. Chung)

2.3.3 Production of PDMS Microchannel Devices

Before PDMS curing, the wafers were treated once with trimethylchlorosilane (Sigma-Aldrich, St. Louis, MO). A few drops of the surface treatment were incubated with the wafers in a vacuum chamber for several hours. This treatment increases the wafers' lifespan by preventing PDMS from adhering to the wafers and peeling off the pattern.

PDMS was prepared by mixing a solution of 1 part by weight curing agent to 10 parts PDMS prepolymer (SYLGARD 184 Silicone Elastomer Kit, Dow Corning, Midland MI). After thorough mixing, the solution was incubated in a vacuum chamber for 20-30 minutes to remove trapped air-bubbles. The PDMS was then poured on top of the wafer and placed in the oven at 80°C for 2-3 hours to cure (Figure 4).

After the PDMS had cured, it was carefully peeled away from the master wafer, and individual chips were excised with a razor blade. Holes were bored in the PDMS chip using a 1.5 mm dermal biopsy punch in order to create fluid inlets to the gel-filling channel, cell chamber and chemoattractant channels. A larger hole-punch was used to create the media well in the second layer of PDMS.

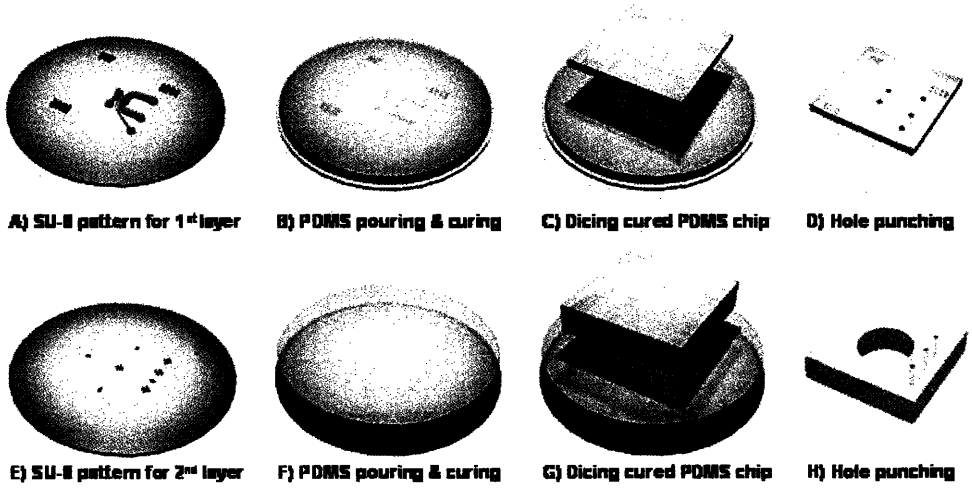

Figure 4. PDMS Preparation and Pouring. PDMS elastomer is first poured over the SU-8 pattern and allowed to cure. Cured chips are then cut and peeled away from the pattern. Holes are punched to fluidically connect the first and second layers and for the media well. (Image courtesy of S. Chung).

In order to complete construction of the device, the two PDMS layers were bound to each other and to a 22 mm square glass coverslip. First, the first layer of PDMS and the coverslip were subjected to plasma oxidation for one minute in a plasma cleaner and sterilizer (Harrick Scientific Corporation, Ossining, NY). Immediately after treatment, the two surfaces were placed into contact, forming a permanent bond. The second layer of PDMS was then treated with the upper surface of the first PDMS layer, and these two surfaces also formed a permanent bond. (Figure 5)

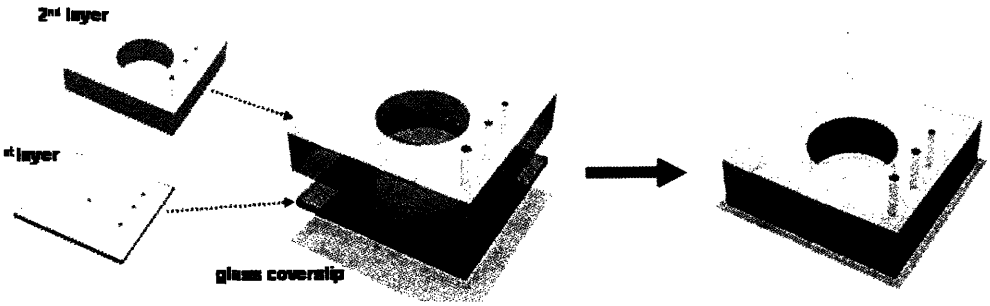

Figure 5. Bonding and Assembly of PDMS Device. The two layers of the PDMS device are bound to a glass coverslip after surface treatment with oxygen plasma. Once the surfaces have come in contact, they cannot be easily detached. (Image courtesy of S. Chung).

2.4 Neuron Culture in PDMS Device

2.4.1 Matrix Materials

The axon channel was filled with collagen prepared at various concentrations in 10x PBS and water. An appropriate volume of NaOH was added to bring the gel to pH 7.35.

2.4.2 Growth Factors and Chemoattractants

In these studies, growth factors known to promote axon outgrowth in CSMN were used as chemoattractants to guide neurites through the channel. The following growth factors were diluted to 50 - 100 ng ml^{-1} in CM and added to the chemoattractant channel alone or in combination: IGF-1, BDNF, CTNF, NT-3, NT-4, and bFGF. We chose this concentration because IGF-1 has been shown to provoke a significant response in pure CSMN at concentrations in this range when applied directly to culture media.[18]

2.4.3 Neuron Culture in Collagen Suspension

The cell culture process in the device is simple, and described in Figure 6. Completed chips are sterilized first by wet autoclave in 1 L dH_2O for 20-25 minutes, then by dry autoclave in an empty pipette tip box for 20-25 minutes (followed by a 15 min dry cycle). If there was still water in the channels after the dry autoclave had completed, chips were placed at 80°C for 5-10 minutes until all liquid had evaporated.

All devices were kept at -20°C for 10-15 minutes before gel filling so that all surfaces would be cold when gel was added, preventing premature polymerization. Gels were loaded by injecting 2-4 µL of pre-gel solution into the chip through a small port in the gel-filling channel with a 20 µL pipette tip. Gel flow was stopped at the ends of the axon channel by capillary forces. Once filled, chips were placed into an empty pipette tip box and allowed to polymerize for 30 minutes in 37°C. Approximately 50 mL sterile H_2O was kept in the bottom of the box as an extra source of humidity during polymerization to prevent the gels from drying out before cells could be added.

After polymerization was complete, approximately 15 mL of chemoattractants and growth factors were loaded through fluid ports at the ends of the channel. Finally, dissociated cells in a collagen suspension were gently loaded into the cell chamber, and

this gel was allowed to polymerize in the humidified chamber at 37 °C for 10 minutes. Media was then added to the media well of the device, and chips were placed into the wells of 6-well plates with sterile H_2O added to the interstitial space between the wells to prevent media evaporation. Neurons were cultured in these devices for up to 7 DIV before they were fixed and stained (see section 2.5).

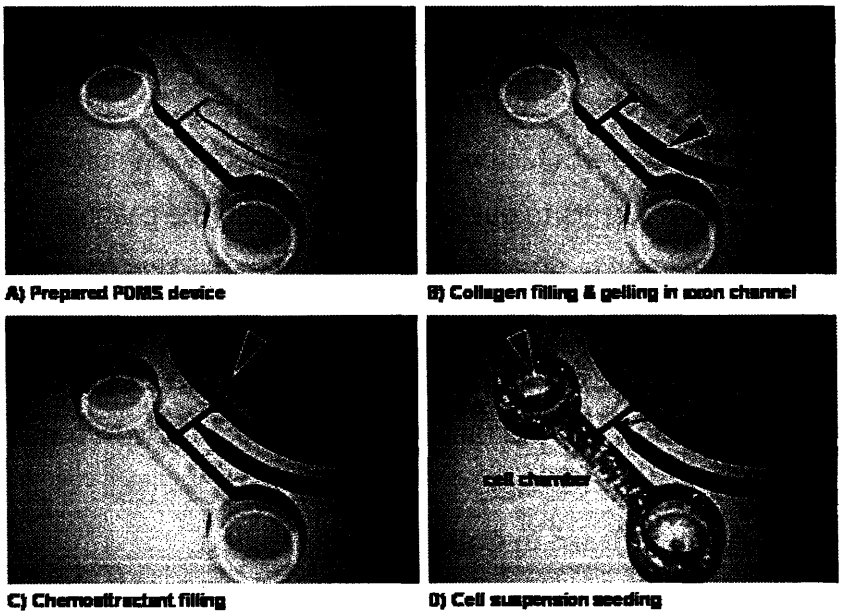

Figure 6. Cell Culture in PDMS Device. The fabricated chip (A) is first sterilized by autoclave and then kept at -20°C before the experiment. Collagen is introduced through the gel-filling channel (B) and allowed to polymerize at 37°C in a humidified chamber. Next, the chemoattractant channel is filled with chemoattractant or growth factor (C). Finally, the cells (in a collagen suspension) are added (D), and after polymerization at 37°C, media is filled in the cell-culture well. (Image courtesy of S. Chung)

2.4.4 Neuron Culture on Poly-L-Lysine Surfaces

In some experiments, we plated cells in the device in media rather than in collagen suspension. Neurites were still directed through a three-dimensional matrix in the axon channel, but the cell bodies were allowed to attach directly to a Poly-L-Lysine (PLL) coated surface. Two methods were used to get PLL inside the cell culture chamber: a cover-slip that was pre-coated with PLL before device assembly, or coating the inside of the channel(s) with PLL solution after device assembly.

PLL coated surfaces cannot support cell adhesion after wet autoclaving (data not shown), so to use a PLL-coated surface as part of the device, the two PDMS layers were bonded and wet autoclaved without the coated cover-slip. Devices were kept in the oven at 80°C until all remaining liquid had evaporated, then the two PDMS layers were

bonded to the coated cover-slip. PLL coating did not affect the strength of the plasma bond between PDMS and the glass. The completed device was then dry autoclaved in an empty pipette tip box as previously described.

Alternatively, some chips were incubated with PLL solution overnight. This technique also coated the PDMS sides of the channels, so it was not unusual to find cells attached to both the top and bottom of the cell culture chamber in these devices. After bonding and autoclaving devices, PLL solution (0.01 mg ml^{-1}) was filled in all of the channels, and the device was left in the incubator at 37°C overnight. In the morning, coating solution was removed, channels were filled with ddH_2O, and chips were incubated for 1-2 hours at 37°C. Liquid was then aspirated from the channels and devices were kept at 80°C until all remaining droplets inside had evaporated.

For both of these coating techniques, collagen was filled in the axon channel as described in section 2.4.3. After the gel had polymerized, fresh media was added to the cell culture chamber and to the chemoattractant channel, and the gel was allowed to equilibrate with the media for up to 12 hours. After dissociation, cells were loaded into the device in suspension in media, and were allowed to attach to the coated surface for 10 minutes. Media was then added and culture proceeded as described above.

2.5 Imaging of Devices

During culture, cells were imaged every 24 hours with phase contrast microscopy in order to more carefully monitor axon extension within the device. After 3-7 DIV, cells were fixed with 4% paraformaldehyde (PFA) and stained with rhodamine-phalloidin (for actin) and DAPI (for DNA). Devices were imaged with a Zeiss inverted microscope equipped with fluorescence optics and high resolution oil-immersion objectives. For a complete sample preparation and imaging protocol, see Appendix D.

3.0 RESULTS

3.1 Optimization of Cell Culture Techniques

Neurons are widely recognized as one of the most difficult cell types to grow and maintain in culture, largely because they are exquisitely sensitive to small changes in their environment (ie: pH, serum levels, presence of other cells, etc.). Growing any type of cell in a PDMS microfluidic system is challenging, and we wanted to ensure that our culture conditions were optimal before introducing cells into the device. Because they were more readily available, all optimization experiments were performed with P0-P1 rat cortical dissociates.

3.1.1 Methods for Cortical Dissociation

Three procedures were evaluated for the tissue dissociation procedure: enzymatic dissociation with Trypsin or Papain, and dissociation with EDTA. Trypsin is the standard protease used to passage cell lines; however, it can create a harsh environment during treatment, and cells exposed to Trypsin for too long are prone to rupture and death. As a gentler treatment, cells were exposed to Versene (0.2 g/L EDTA in PBS, Gibco), a chelating agent. Because many cell-cell interactions are mediated by calcium, treatment with Versene could gently dissociate the tissue without causing cells to rupture from over-digestion. Finally, Papain, a different protease, is gentler than Trypsin, and is widely used for dissociating neural tissue.

Enzyme solutions were allowed to equilibrate to the proper pH and temperature in the incubator for approximately 30 minutes. Tissue pieces were then incubated with filtered Trypsin (10 minutes), Versene (30 minutes) or Papain (15-30 minutes). All three treatments regularly produced healthy neurons (Figure 7), but Papain-treatment consistently produced the highest yield of viable neurons and the longest extensions. Further experiments were conducted using Papain, as described in section 2.1 and Appendix B.

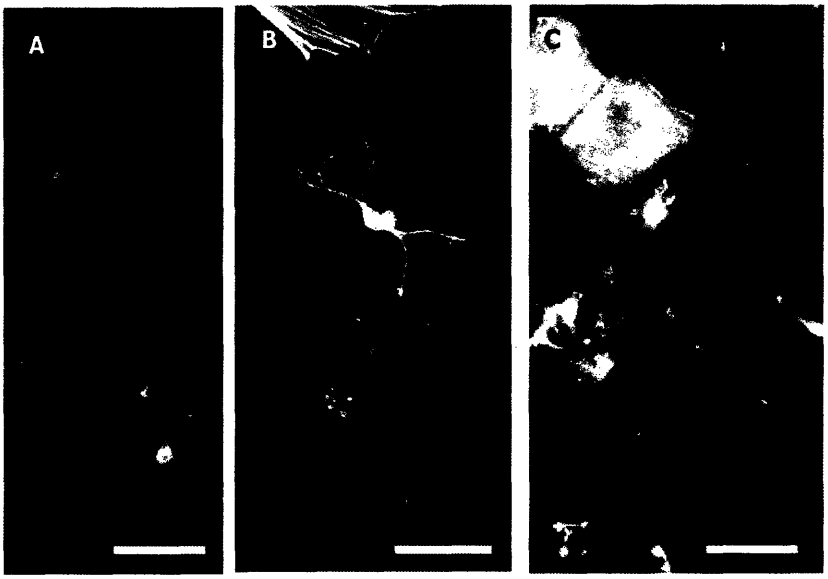

Figure 7. Optimization of Dissociation Technique. Representative images of P0-P1 rat cortical cells dissociated with Trypsin (A), Versene (B) and Papain (C). Cells were plated at a density of 10^6 cells/ml in all cases. While all three treatments could be used successfully, Papain dissociations consistently produced the longest extensions and the highest neuron viability. Often, extensions were entangled with each other and difficult to trace separately. Cells were grown for 6 days and stained for actin (yellow) and nucleus (blue). Scale bar 50 μm.

3.1.2 Cell Culture Media and Cell Density

Neurons typically grow best at higher cell densities (approximately 10^6 cells ml^{-1}), presumably due to astrocytes and glial cells that secrete growth-promoting molecules[29]. We were most interested in growing cells in our devices at a relatively low density for many reasons, including ease of imaging and ability to track the effects of signals or growth factors on single cells. Thus, we needed to develop an effective protocol for low cell density culture of neurons.

Media serum levels and conditioned medium were evaluated for their ability to support axon outgrowth of neurons grown at relatively low densities (10^4 cells ml^{-1}). Cells were plated in medium containing 5%, 10% and 15% FBS, as well as conditioned medium (CM, 10% FBS) conditioned overnight on mixed cortical cells. While all four culture media promoted cell survival and axon outgrowth, cells were consistently the healthiest in the 10% serum condition. Cells grown in CM also often had longer axons than those in fresh medium. Presumably, the conditioning introduced beneficial growth factors and other molecules secreted by mixed cortical cells, thereby compensating for the low cell density in culture (Figure 8).

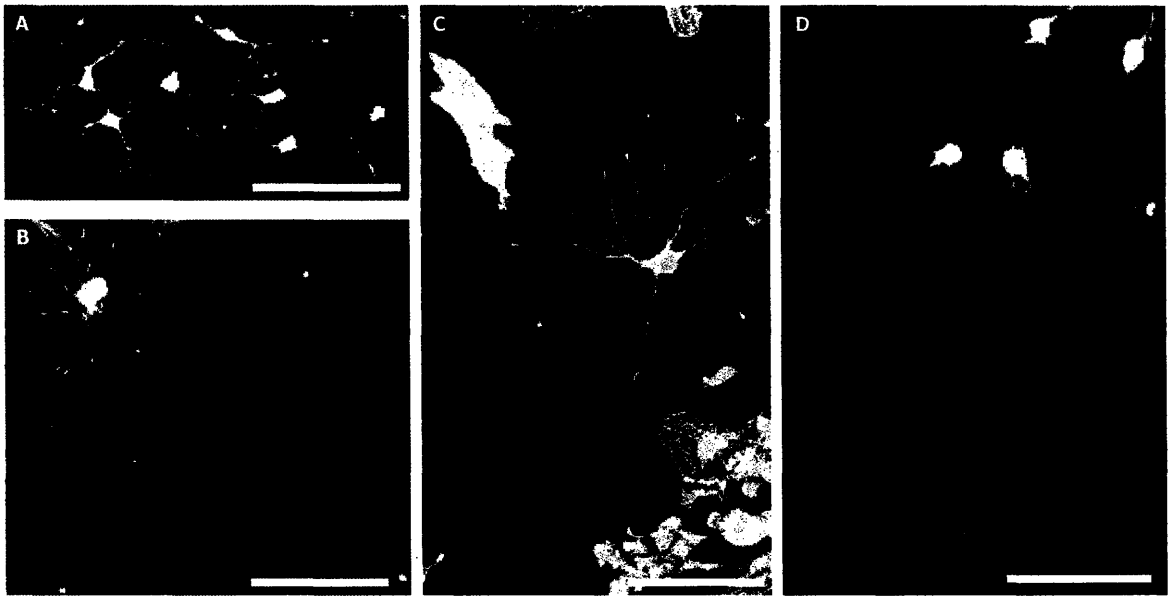

Figure 8. Optimization of Media for Low-Density Neuron Culture. Representative images of P0-P1 rat cortical cells grown in media with serum levels of 5% (A), 10% (B), and 15% FBS (C), as well as conditioned media (CM, 10% FBS) (D). The 10% serum condition consistently produced cells with the longest axons, and conditioning the media overnight (as in D) also promoted axon outgrowth. Cells were grown for 6 days and stained in rhodamine-phalloidin (actin, yellow) and DAPI (nucleus, blue). Scale bar 100 μm.

3.1.3 Collagen Preparation

In these experiments, our aim was to determine the concentration of polymerized collagen that would be firm enough to maintain its microarchitecture within the device while remaining soft enough to allow axon outgrowth. Cells were plated in collagen in 24-well plates prepared in CM at concentrations ranging from 0.5 mg ml^{-1} to 2.0 mg ml^{-1}, and were placed at 37° for 10 minutes. After the collagen polymerized, the cells were covered with SCM, and cell survival and axon outgrowth were monitored for two days. As a control, neurons were plated on poly-L-lysine coated cover-slips, a standard method for neuronal cell culture. After two days, it was clear that the cells embedded in collagen at 0.5 mg ml^{-1} were healthy and had extended neurites equivalent to those cultured on poly-L-lysine (Figure 9). Neurite length visibly decreased as the collagen concentration increased to 2.0 mg ml^{-1}, suggesting that higher concentrations of collagen are simply too stiff or too dense for axon outgrowth.

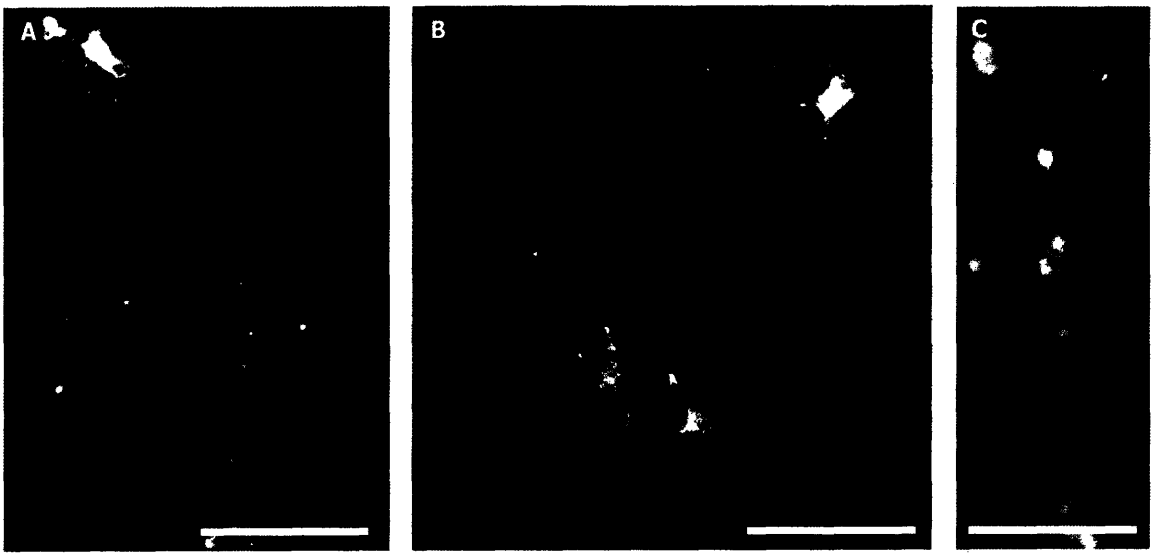

Figure 9. Dissociated Cortical Cells in Culture. P0-P1 rat cortical dissociates were cultured either on the flat surface of a cover-slip coated with poly-L-lysine (A) or embedded in type-I collagen in concentrations of 0.5 mg ml^{-1} (B) to 2.0 mg ml^{-1} (C) prepared in CM. Mixed dissociated cells demonstrated proper axonal outgrowth in both cases, but only collagen allowed three-dimensional growth in culture. Axon length visibly decreased as collagen concentration increased from 0.05% to 0.2% wt/vol. Cells were grown for 6 days, fixed, and stained for actin (yellow) and nucleus (blue). Scale bar 100 μm.

3.1.4 Collagen Interfaces

Our device design requires that cells send an axon into a collagen matrix different from that in which they are cultured. The axon must cross an interface in order to grow into the axon channel where the chemoattractant gradient exists. We wanted to ensure that growth cones were not discouraged by the presence of an interface between two gels. We first allowed a cell-free dot of collagen (concentrations from 0.5 to 2.0 mg ml^{-1}, prepared in CM) to polymerize on the bottom of a 24-well plate. A suspension of neurons in 0.5 mg ml^{-1} collagen prepared in CM was then spotted next to the cell-free collagen and allowed to polymerize. The well was then filled with CM and kept in culture for 6 days before cells were fixed and stained.

We found that neurons were easily able to send long axons (~500 μm) into low concentration gels of 0.5 mg ml^{-1} (Figure 10). Interestingly enough, these neurons were also able to send relatively long axons (~300 μm) into high concentration gels of 2.0 mg ml^{-1}, despite the fact that no projections longer than 100 μm were seen when cells were embedded in gels of this concentration (as in Section 4.1.3). This discrepancy may be due to differential expression of integrin receptors or matrix proteases in the cell body

as opposed to the axon, or perhaps an inability to generate an axon in gels of high concentration. In any case, projections were capable of crossing collagen gel interfaces of the same or different concentrations, though lower concentrations consistently yielded longer axons.

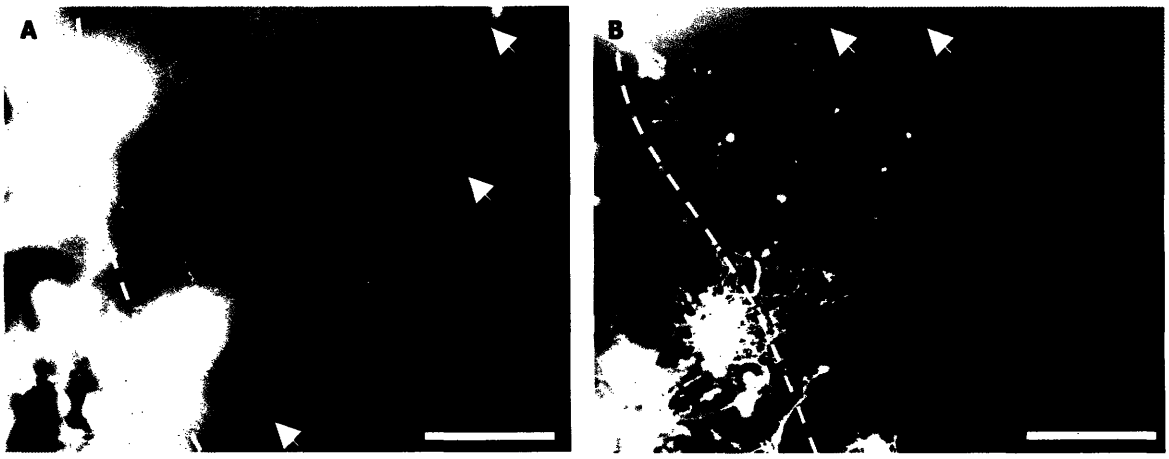

Figure 10. Axons crossing collagen interfaces. P0-P1 rat cortical cells were suspended in 0.5 mg ml^{-1} collagen and axons were allowed to project into cell-free collagen of 0.5 mg ml^{-1} (A) or 2.0 mg ml^{-1} (B). The gel interface in the plane of focus is shown as a dashed white line. Some fluorescence interference from higher or lower focal planes is seen at the interface, though cell bodies were completely confined to the left side of the image. Although axons were able to cross into both gels, projections were consistently longer in the lower concentration gels. Scale bar 100 μm.

3.1.5 Cell Culture Protocol Conclusions

From the results of these optimization studies, we concluded that postnatal cortical cells should be dissociated with the protease Papain and cultured in conditioned medium containing 10% serum. Cells will also be grown in the device on PLL or suspended in 0.5 mg ml^{-1} collagen solution prepared in CM. Ideally, the axon channel should also be filled with collagen at 0.5 mg ml^{-1}, but axons are capable of penetrating long distances into gels with concentrations as high as 2.0 mg ml^{-1}.

3.2 Device Design Modifications

The microfluidic system used in these experiments was designed with the following goals: optimize cell survival, apply a stable gradient of chemoattractant, and promote axon growth through a three dimensional matrix material. Our design consists of three basic parts: a chamber for cell culture, a chemoattractant channel that functions as a constant source of growth factors, and an axon channel that connects these two structures. Liquid ECM gel components are flowed into the axon channel through a gel-filling channel. The flow of liquid is stopped at the ends of the axon channel by capillary forces, and the gel is allowed to polymerize before cells are introduced. To create flexibility in the experiments, several different designs were patterned onto the silicon wafer. Some chips had two axon channels leaving the same cell culture chamber, and the axon channel varied in length from 600 μm to 1 mm.

In our original design (Figure 11), the cell culture chamber was simply a hole that was fluidically connected to the axon channel and a reservoir of media. While this approach made it easy to introduce cells in a gel suspension into the system, the uneven interface of the punch obstructed imaging of the entrance to the axon channel, a critical region of the device.

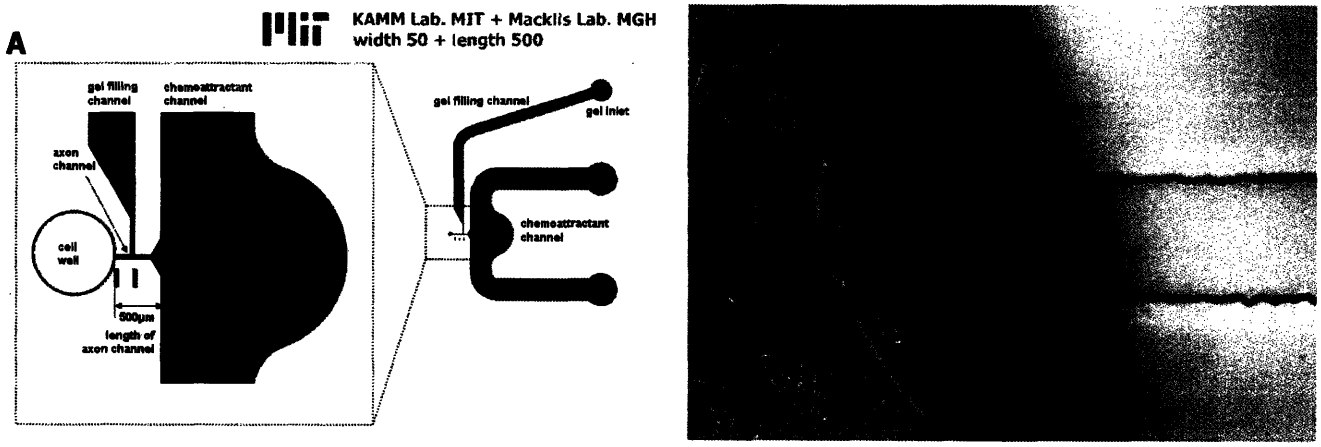

Figure 11. Preliminary Design of Microfluidic Device. Preliminary device design is shown in (A). Neurons were cultured in the cell culture well, and axon outgrowth was directed through the collagen gel in the axon channel by a gradient of chemoattractant. An image of P1 mouse cortical cells in the finished PDMS device is shown in (B). Unfortunately, the critical junction between the cell culture chamber and the axon channel is difficult to visualize because of the uneven PDMS boundary. (Channel design image courtesy of S. Chung).

In response to these weaknesses, we revised the design of our system such that cells were introduced into a chamber connected to the media well by two ports (Figure 12). This design had no adverse effect on efficiency of gas exchange, and waste removal was not compromised because the gel within this chamber had two interfaces with the media, allowing rapid diffusion of nutrients from both directions. Neurite extension was still directed down an axon channel, but the intersection between the cell culture chamber and the axon channel was smooth, allowing clearer and more informative images. In addition, the gel in the device was more stable and easier to fill because the height of the axon channel was much less than the height of the chemoattractant channel or cell chamber.

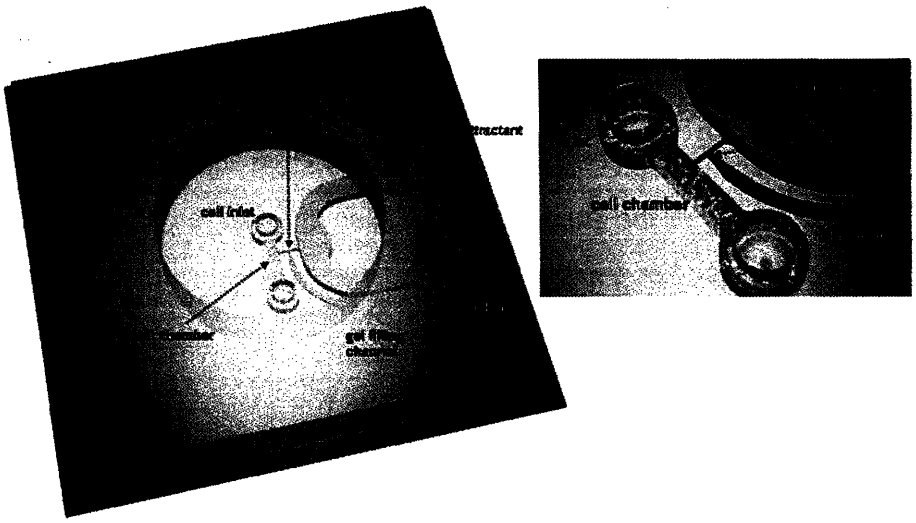

Figure 12. Microfluidic Device for Improved Imaging. Our second design made the interface between the axon channel and the cell chamber easier to visualize. In addition, the gel in the axon channel was more stable and easier to fill because of the height difference between the axon channel (12 μm) and the cell chamber or chemoattractant channel (100 μm). (Image courtesy of S. Chung)

While this second device greatly improved imaging capabilities, we still encountered problems with gel stability and inhomogeneous polymerization. If any fraction of the pre-gel solution began to polymerize before reaching the axon channel, the device had a non-uniform concentration. Even with extremely careful preparation where all devices and instruments were kept at -20°C before coming in contact with the collagen, cells and cellular debris were able to flow around the patches of polymerized collagen. At first, it appeared that we were operating with collagen below a critical gelation concentration, but gels with concentration as high as 3.0 mg ml^{-1} were still unable to polymerize evenly in the 12 μm axon channel (data not shown).

In short, the problem was most likely that the axon channel height was comparable to the pore size of the collagen gel in the channel. While a type I collagen molecule is only a few nm in diameter, a polymerized matrix has fibrils 50-200 nm in diameter[30], and in a reconstituted hydrogel of type I collagen at 5 mg ml^{-1}, typical pore sizes between fibrils are on the order of 1 μm[31]. Decreasing collagen concentration to 2.0 mg ml^{-1} or less primarily lowers the density of fibrils in the matrix, effectively increasing pore size[32]. Because the axon channel height was only 12 μm, the approximation of the gel as a continuum was not valid, and the matrix likely behaved as a discrete arrangement of collagen fibrils rather than a continuous gel. By increasing the height of the axon channel to 50 μm, the axon channel was large enough to contain a polymerized meshwork of collagen fibrils capable of excluding cell bodies and debris and establishing a diffusive gradient of growth factor between the chemoattractant channel and the cell culture chamber.

Another gel stability issue that we encountered was that gel shrinkage after polymerization and evaporation created pressure gradients within the device causing fluid and small cellular debris to flow into the gel filling channel when cells and media were introduced (see Figure 13). This problem was addressed by loading gel through a small hole (less than 500 μm inlet diameter) in the middle of the gel filling channel instead of the larger port at the end of the channel. The pressure was equalized at both ends of the gel-filling channel because this hole was completely covered by media. In addition, the small inlet diameter prevents large surface tension forces from being generated by the curvature of the fluid at the port and also serves as an additional diffusive source of media and nutrients to the axons in the device.

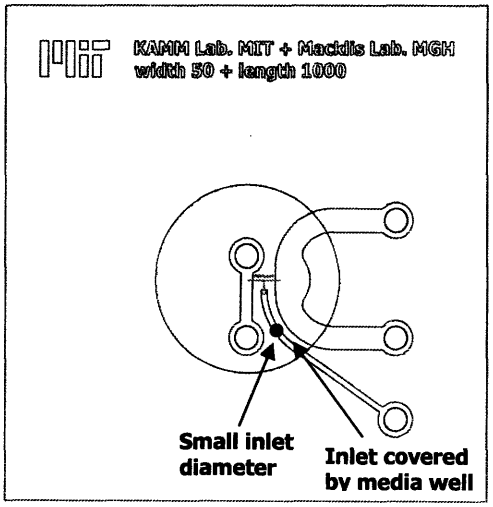

Figure 13. Device Improvements to Remove Pressure Gradients. After polymerization, fluid often evaporated from the gel-filling port (which was not covered by any sizeable amount of media. This evaporation established a pressure gradient along the gel-filling channel. Pressure gradients were virtually eliminated after the addition of a small hole in the gel-filling channel. (Image courtesy of S. Chung).

3.3 Gradient Modeling

Before experimentally testing the gradient in the device, we modeled our system qualitatively and in FEMLAB in order to get an idea of the expected gradient shape and the time scale of gradient development. We consider the axon channel as two separate regions – before and after the gel-filling channel. In addition, because a substantial amount of chemoattractant flux will go up the gel-filling channel, its presence cannot be neglected. The geometry of transport as well as the governing equation and boundary conditions can be found in Figure 14. We make the following additional simplifying assumptions:

1) The diffusion coefficient, D, remains constant in all three regions.
2) There are no pressure gradients or fluid flows in the device; all transport occurs by diffusion.
3) Transport is one-dimensional in each region.
4) Concentration in the chemoattractant channel remains constant at C_0 over the course of the experiment.
5) Concentration in the cell culture chamber remains at zero. The chamber volume is much larger than the axon channel volume, and it is connected to the large, open media reservoir at two ports, so any chemoattractant build-up in the cell culture chamber will be extremely dilute.

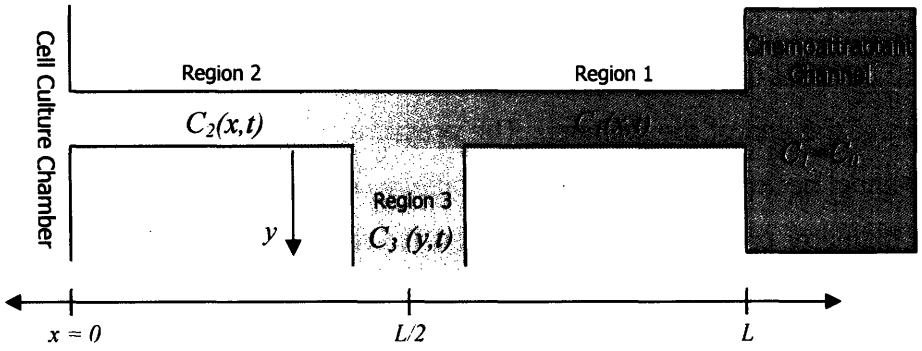

Governing Equation

$$\frac{\partial C}{\partial t} = \frac{\partial^2 C}{\partial x^2} + \frac{\partial^2 C}{\partial y^2}$$

Initial Condition

$t = 0 : C_1 = C_2 = C_3 = 0$

Boundary Conditions

Region 1

$x = L/2$:

$$DA_1 \frac{\partial C_1}{\partial x} = DA_2 \frac{\partial C_2}{\partial x} + DA_3 \frac{\partial C_3}{\partial y}$$

$x = L : C_1 = C_0$

Region 2

$x = 0 : C_2 = 0$

$x = L/2 : C_1 = C_2$

Region 3

$y = 0 : C_3 = C_2$

$y \to \infty : C_3 \to 0$

Figure 14. Schematic of Transport in the Axon Channel. The device can be broken into three regions in which diffusion occurs in one-dimension only. Region 1 extends from the chemoattractant channel to the gel-filling channel. The concentration in region 1, C_1, is dependant only on x and t. Region 2 is the rest of the axon channel, and C_2 also depends only on x and t. Region 3 is the gel-filling channel, and C_3 depends only on y and t. The diffusion equation thus applies in only one dimension in each of the three regions. Boundary conditions for each region and the initial condition are shown to the right.

Obvious boundary conditions are the constant concentrations at $x = 0$ (cell chamber) and $x = L$ (chemoattractant channel). Additional boundary conditions apply at $x = L/2$: the concentration profile must be continuous (in all regions), and the diffusive flux coming from region 1 must equal the flux entering regions 2 and 3. Finally, because the gel-filling channel is also connected to the media reservoir at its port, we assume that its concentration drops to zero at high values of y.

The steady-state solution to the one-dimensional diffusion equation in a single channel with fixed concentrations at both ends is a homogenous linear profile. Qualitatively, we expect that in our device, the steady-state profile will also be linear in both regions of the axon channel. Upon reaching the second region, the chemoattractant molecules will either be transported up the gel-filling channel (region 3) or continue through the axon channel to the cell culture chamber (region 2). Because their cross-sectional areas are roughly equal, these two paths should be equally likely, so roughly half of the chemoattractant flux from region 1 will enter each region 2 and 3. As a result, we expect that the gradient in region 2 of the axon channel will be approximately half as steep as in region 1.

To verify these qualitative estimates, we used FEMLAB, a finite-element modeling software that allows simulation of transport processes. We first drew the channel geometry to scale in the unsteady diffusion module of the program, and specified the boundary conditions as in Figure 14. As in our experiments, the axon channel was 600 μm long and 50 μm wide. All PDMS walls were set to be insulating (no diffusive flux). The results of this simulation are shown in Figure 15. Transient gradients develop first in region 1 of the axon channel, but spread into region 2 within approximately 20 minutes. According to the simulation, steady state is reached after approximately 2.75 hours (10,000 seconds).

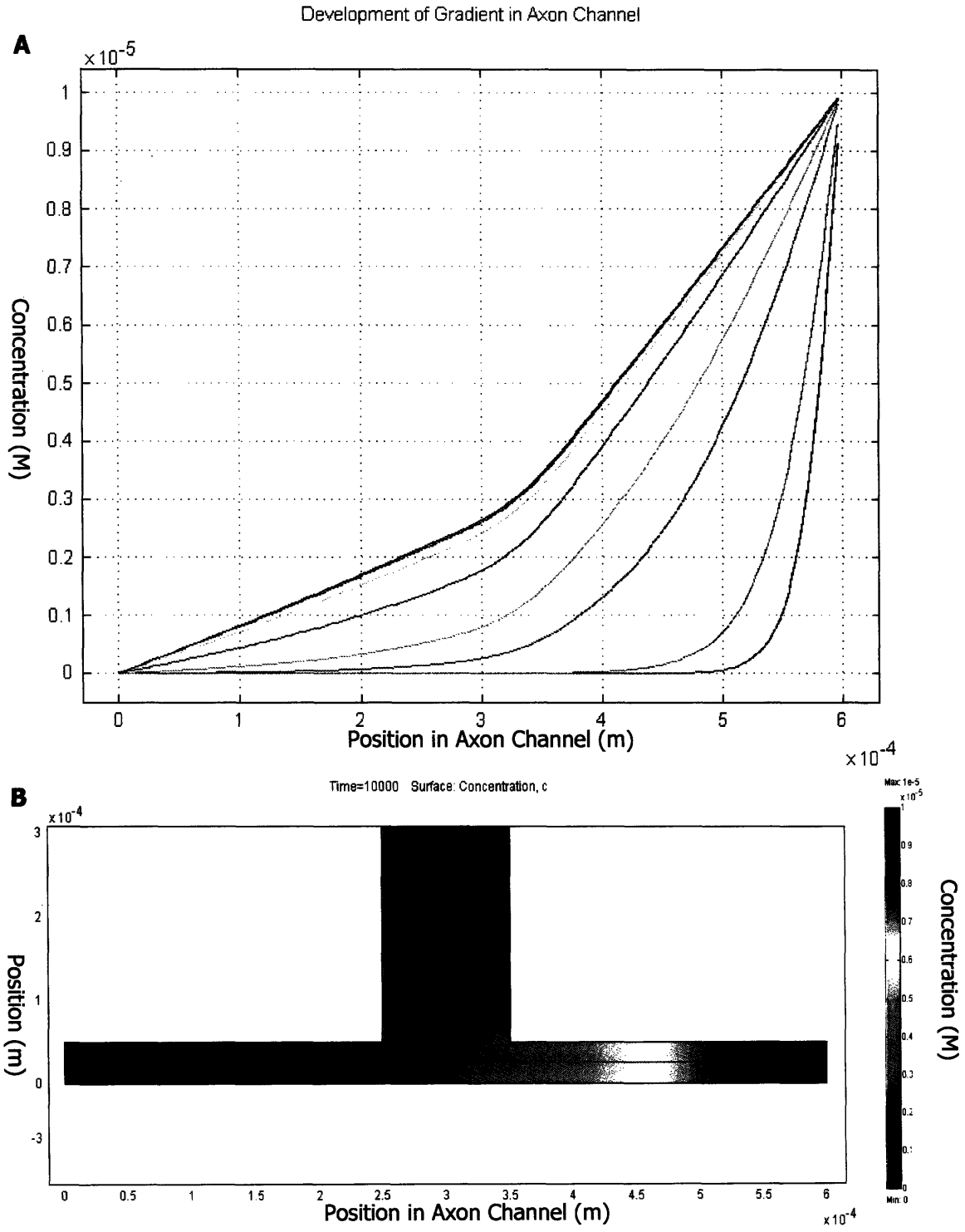

Figure 15. Finite Element Modeling of Gradient Transients in the Axon Channel. Simulations were performed in FEMLAB for a constant concentration at the chemoattractant channel and zero concentration at the cell culture chamber. Developing transient concentration profiles in the center of the axon channel are shown in (A). The eight time points shown are: 50, 150, 1000, 2150, 4950, 8300, 9700, and 10000 seconds. The steady-state profile (B) is reached after approximately 10000 seconds, or 3.75 hours.

3.4 Gradient Testing in PDMS Device

In order to verify the presence and sustainability of a chemical gradient through the axon channel of our device, we needed a fluorescently labeled probe with similar properties as the chemoattractants and growth factors of interest. Common probes include small dyes conjugated directly to the protein of interest or fluorescently labeled molecules with similar diffusion behavior. We chose to use FITC-labeled dextran as a tracer for these experiments because it can be acquired in any molecular weight, thereby having the diffusion characteristics of any arbitrary protein. Since IGF-1 was the most commonly used chemoattractant in our studies, we looked for a FITC-dextran that would approximate its diffusion behavior in solution.

IGF-1 is a 57-residue peptide with a molecular weight of 7 kDa. Nauman et al. studied the diffusion behavior of IGF-1 at 25°C in the absence of binding, and they report a value of $D = 1.59 \times 10^{-6}$ cm^2 s^{-1} for the diffusion coefficient of IGF-1 in low molecular-weight hydrogels.[33] A 10 kDa FITC dextran was readily available, with a diffusion coefficient of $D = 9 \times 10^{-7}$ cm^2 s^{-1} as reported by fluorescence recovery after photobleaching.[34,35] The gels in our devices are of sufficiently low concentration that they can be approximated as a dilute solution.

All devices were prepared and analyzed as described in Section 3.3. Collagen at 2.0 mg ml^{-1} was allowed to gel in the axon channel, and PBS was added to the cell chamber of the device. FITC-labeled dextran (10 μM in PBS) was then added to the chemoattractant channel, and fluorescence images were taken at various time points. During the experiment, chips were kept in a humidified Petri-dish, and movement from the microscope stage was minimized as much as possible. Images of the axon channel were cropped using NIH Image J software, and analyzed in MATLAB. Briefly, pixel values were normalized by subtracting the background light from a sample without the tracer, and then divided by the maximum pixel value of 10 μM tracer. An average was then taken across each cross-section of the axon-channel image, and this value was plotted against its position in the channel. Appendix E contains relevant MATLAB code for gradient quantification. Normalized concentration values for a gradient-testing experiment are shown in Figure 16.

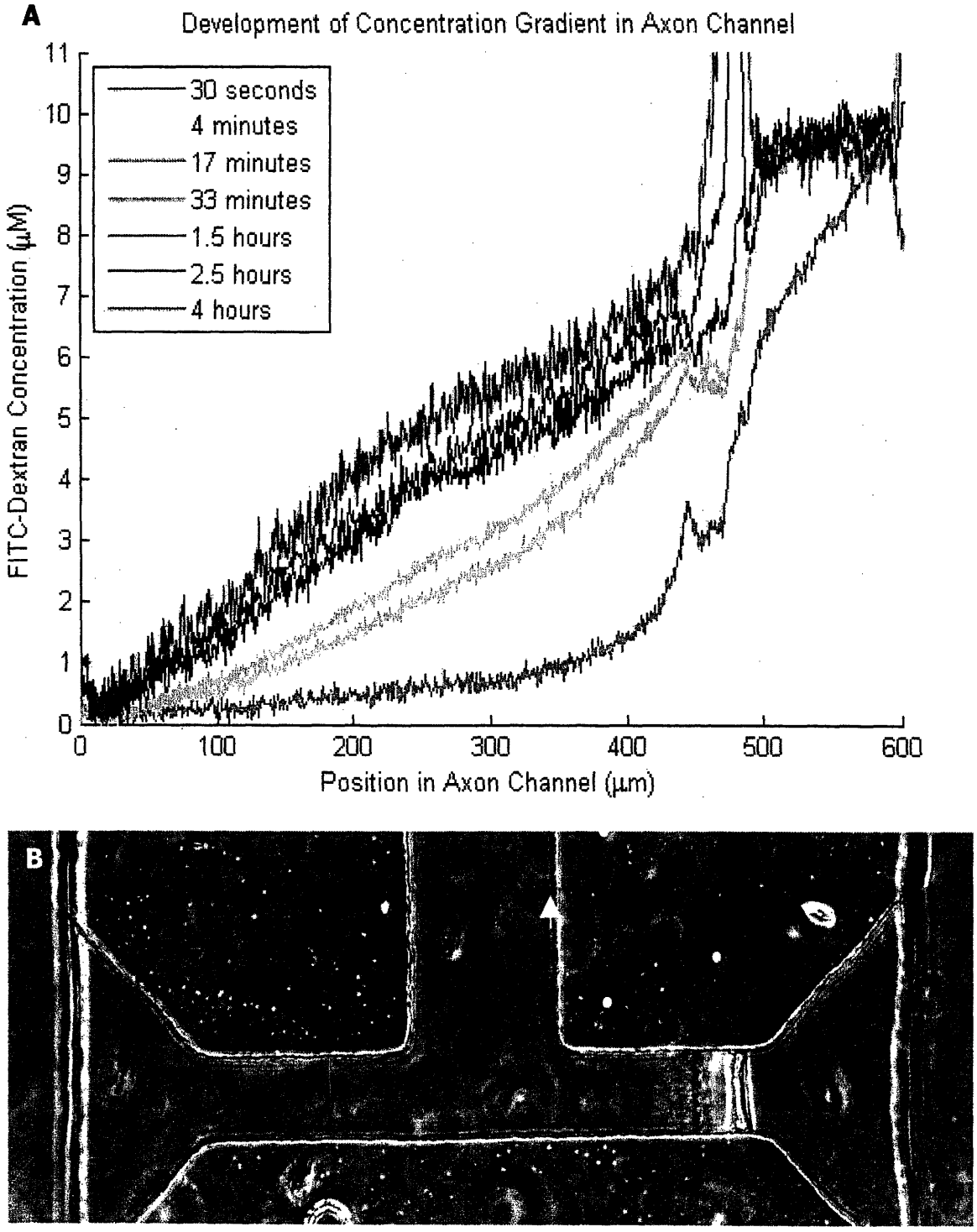

Figure 16. Development of a Concentration Gradient of Chemoattractant in the Axon Channel. FITC- dextran (10 μM) was used as a tracer to monitor diffusion through the axon channel (A). The concentration at the cell culture chamber was held at zero and the concentration at the chemoattractant channel remained at 10 μM throughout the time-course of the experiment. A crystal-like structure at the beginning of the chemoattractant channel caused a disturbance in the pixel intensity of all gradient images (white arrow, B).

A discontinuity in the gradient can be seen near x = 500 μm along the axon channel. While the MATLAB analysis appears to show a jump in concentration, phase-contrast images (Figure 16B) reveal a crystal-like obstruction, which disrupted the fluorescence intensity in the channel. This obstruction is most likely formed during polymerization as the PBS in the collagen solution began to dry out. We had previously seen this type of obstruction in devices, and it does not appear to affect cell growth into the device (data not shown).

The graph shown in Figure 16A suggests that this crystal is providing a resistance to diffusion. As early as 4 minutes into the experiment, the tapered region of the gel-filling channel between 500 and 600 μm had nearly equilibrated to the concentration of the chemoattractant reservoir, and a step-change in concentration was clearly visible across the obstruction. In spite of this obstruction, a gradient was observed in the channel for long time-points, but to be entirely sure that the gradient is present and stable in other systems, the experiment should be repeated.

It is also important to note that at later time-points, the tracer fluorescence began to decrease, resulting in lower pixel intensity, as seen by the thickness and variation of the lines at later time-points. This phenomenon is likely due to photobleaching of the FITC fluorophor attached to the dextran tracer. Although the sample was only exposed to UV-light during imaging, several hours of time-lapse imaging and frequent exposure to white light for sample positioning is often enough to bleach the FITC fluorophors. Problems associated with this experiment are discussed in subsequent sections, and the results of additional gradient-testing experiments are presented and discussed in Appendix E.

3.5 Cell Culture in PDMS Device

3.5.1 Axon Extension within Device

An important goal of device development was to observe neurites extending into the axon channel. Although there were some initial problems related to optimizing cell culture conditions within the device and gel stability (discussed in previous sections), we quickly discovered that neurons and glial cells grow and proliferate easily within the cell culture chamber. In fact, unless a cell-cycle inhibitor is introduced to the media, glial cells will expand and become confluent in the cell chamber within 6-9 days, just as they do in standard open culture.

Neurons were equally healthy within the device, and rapidly responded to applied gradients of growth factor (Figure 17). Devices were pre-filled with collagen at 2.0 mg ml^{-1} and allowed to equilibrate with conditioned media (CM) overnight. The next day, cortical dissociates from P2 GFP mice were flowed into the cell culture chamber in media suspension, and allowed to adhere to the PLL-coated cover-slip for approximately 30 minutes. The media was then changed and cells were kept in culture for 24 hours. After 24 hours, IGF-1 was added to the chemoattractant channel at a concentration of 100 ng ml^{-1}. Several long (over 400 μm) axons grew into the axon channel overnight, and no neurites were observed extending in the direction opposite the gradient. Devices to which IGF-1 was not added did not exhibit this robust axon extension between 24-48 hours (data not shown), suggesting that the cells were indeed responding to the IGF-1 signal.

Samples were fixed and stained after 48 hours so that high resolution and fluorescence images could be acquired (Figure 18). Staining for actin fibers clearly revealed three long axons in the axon channel, and higher resolution images show many more neurites in various focal planes entering the collagen gel in the axon channel. It is interesting to note that in this experiment, axons began to drift or turn into the gel-filling channel. Several factors could have contributed to disruption of the gradient, including evaporation, sample disruption, or the presence of diffusive resistance. These factors could have caused the gel-filling channel to be indistinguishable from the rest of the gel-filling channel based on the concentration gradient at the growth cone, preventing axons from effectively reaching the chemoattractant channel.

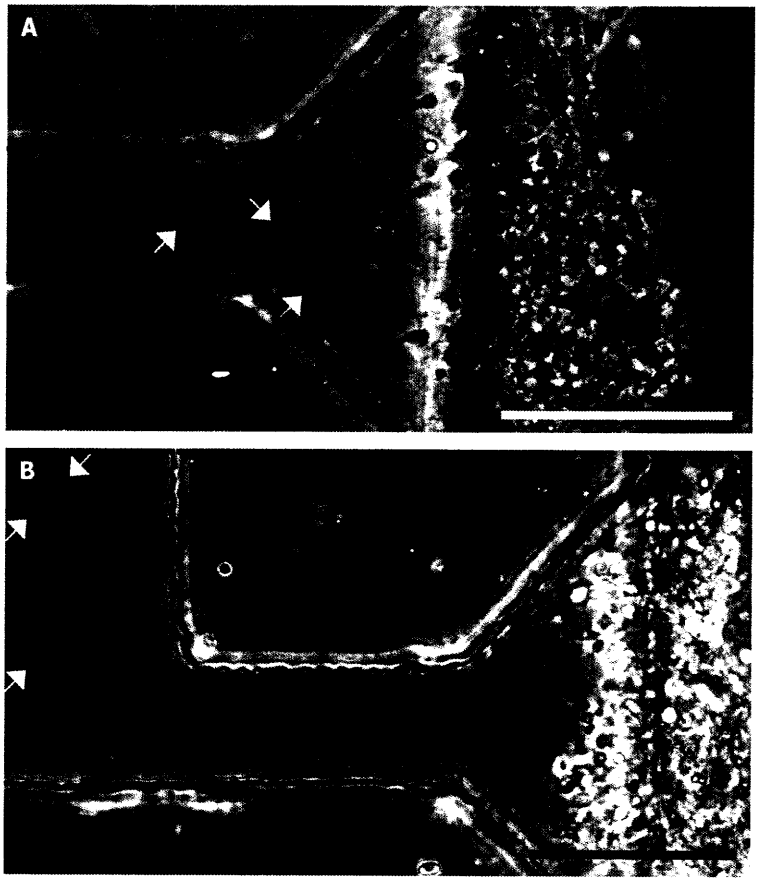

Figure 17. Axon Extension in Response to IGF-1. Mouse cortical neurons were imaged in the device 24 hours after plating (A). IGF-1 (100 ng/ml) was added to the chemoattractant channel immediately after imaging at 24 hours. Robust axon extension was seen through the device 24 hours after application of the gradient. Scale bars 100 μm.

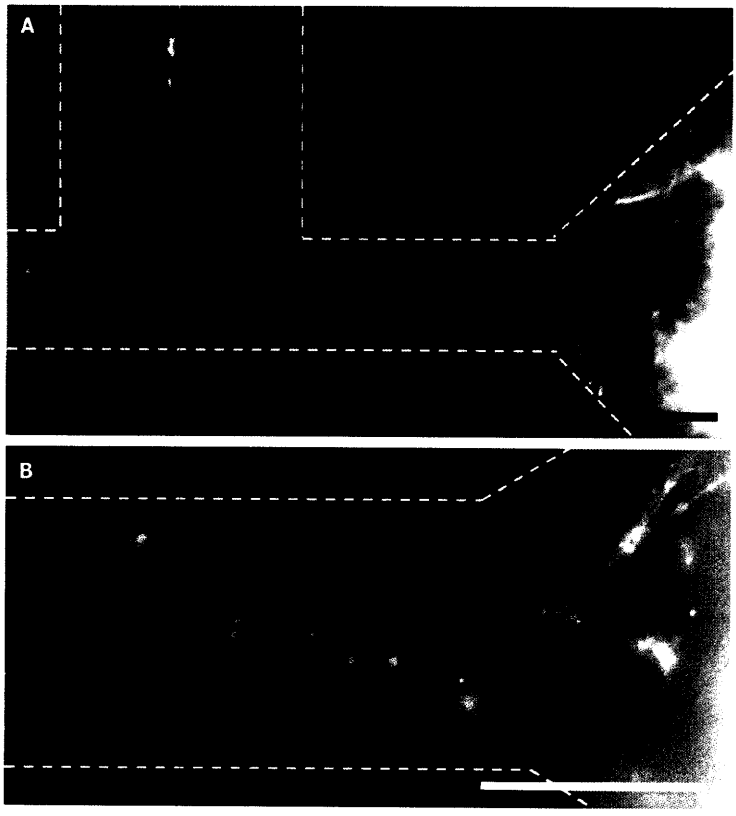

Figure 18. Neurite Extension through the Axon Channel. P2 mouse cortical neurons were fixed 48 hours after plating, and stained for actin (yellow) and nucleus (blue). Axons can be seen in the axon channel and gel-filling channel (A). High resolution (60X) images were also acquired of axons entering the axon channel (B). Scale bars 50 μm.

Figure 19. Neurite Extension into Axon Channel in Response to bFGF. P0-P1 rat cortical cells were cultured in the device, and after five days, an axon several hundred microns long was seen extending over an island of glial cells and into the axon channel in the presence of a gradient of bFGF (A). High resolution imaging of the axon (B) reveals that it follows the PDMS surface of the axon channel. The growth cone can be seen in two dimensions (white arrow). Scale bar: 100 μm in (A), 20 μm in (B).

Long extensions were also seen with neurons in collagen (Figure 19). P0-P1 rat cortical dissociates were plated in the device in a low-density collagen suspension. Although the cover-slip was not coated with PLL, cells appear to have settled before the gel polymerized and spread out on the glass surface. Basic Fibroblast Growth Factor (bFGF) was used as a chemoattractant in this experiment. Although not typically associated with the nervous system, bFGF is well known to regulate glial cell migration and proliferation[36] and has also been shown to play a role in the development of cortical neurons and their ability to extend axons[37].

Cells were fixed and stained for imaging after five days in vitro, and a long axon (over 500 μm long) had extended over the glial cells and into the axon channel. Upon coming into contact with the PDMS of the channel, the growth cone began to follow the rough surface of the wall. Images taken at 60x magnification confirm that the axon follows the PDMS wall and reveal the growth cone in two dimensions. It is interesting to note that this cell does not exhibit typical neuronal morphology: it has a huge cell-body and has spread out on the cover-slip like a large glial cell, yet it has maintained the ability to send axons over long distances in three dimensions. The glial cells near the entrance to the axon channel may have also provided support for the growing axon.

Most likely, the cell would have fully differentiated into a neuron if it had been left to develop *in vivo* in the cortex, but certain environmental signals were removed upon dissociation, leaving a hybrid cell with glial morphology but the ability to send neurites over long distances. It is also likely that this cell's robust response to bFGF is in part due to its hybrid morphology and an ability to respond to the signal in an atypical way.

3.5.2 Cell Migration within Device

Another phenomenon occasionally observed in the device is glial cell migration through the axon channel. As previously noted, bFGF has been shown to cause glial cell migration and proliferation, and migration was most commonly observed when bFGF was used as the chemoattractant (Figure 20). It is possible that some of the cells shown in the axon channel did not migrate into the channel, but were the products of proliferation inside the channel instead. The absence of cellular debris in the axon channel suggests that the gel was intact upon cell-filling and that the cells actively entered the axon channel. Once in the axon channel, some cells turned up the gel-filling channel and others continued to the chemoattractant channel. It is unclear whether the cells completely degraded the collagen in the device or if some of the matrix remained intact. Although the present study is less interested in cell migration, in future experiments, this device could easily be used to track and quantify migration of motile cell types in response to chemotactic gradients.

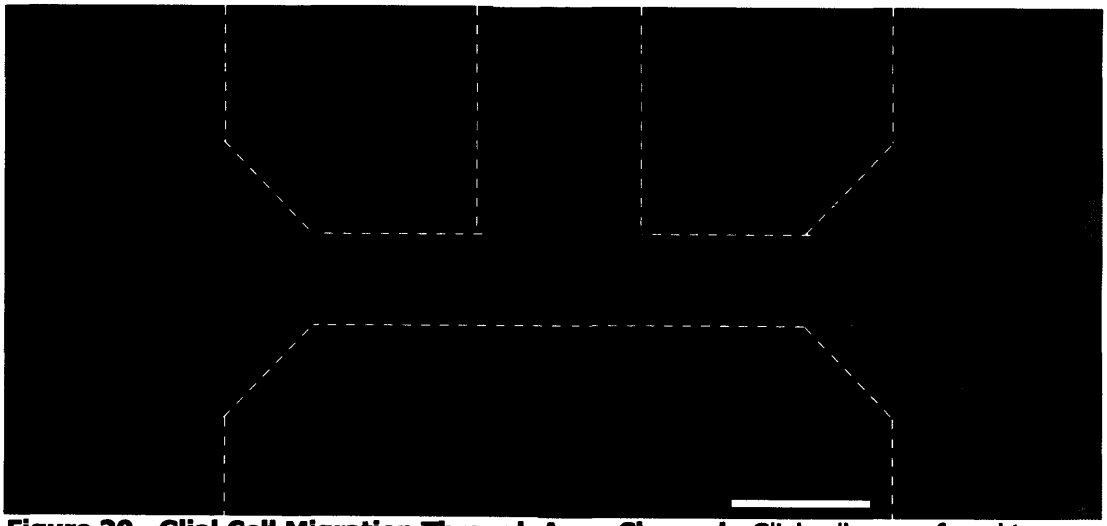

Figure 20. Glial Cell Migration Through Axon Channel. Glial cells were found to migrate into the axon channel in response to bFGF. Cells were grown for 6 days in vitro, then fixed and stained for actin (green) and nucleus (blue). White lines represent channel barriers and orange dotted lines represent the gel interfaces. Scale bar 100 μm.

3.5.3 High-Resolution Fluorescence Imaging of Growth-Cones

One of the most interesting and useful features of our device is its compatibility with high-resolution imaging. Because the axons in our devices were able to remain on the PLL-coated cover-slip or extend through the collagen matrix in the axon channel, we were able to capture images of growth cones in both two and three dimensions (Figure 21). In two dimensions, the growth cone resembles a hand spread out on a surface, and filopodia are only generated on the plane of growth. When it is extending in three dimensions, the growth cone appears more conical in shape, sampling a narrower angle with its filopodia. Images were acquired by both internal GFP fluorescence and an actin stain. It is interesting to note that actin is an integral part of the growth cone's ability to move through its environment, and the stain is much brighter in the filopodia of the growth cone than in the rest of the axon.

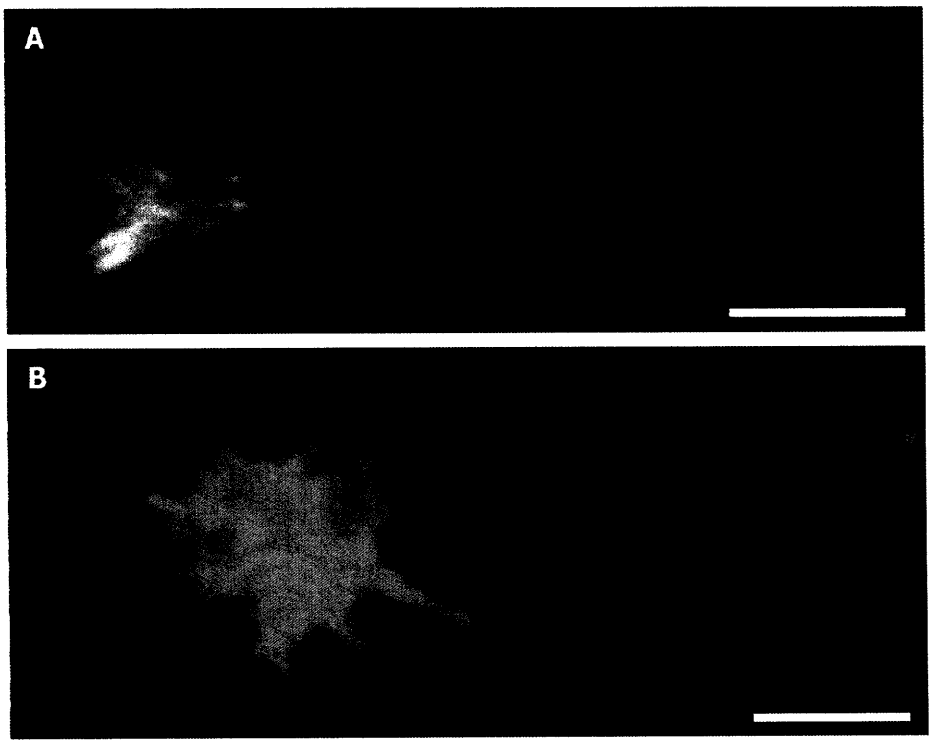

Figure 21. Growth Cones in the Device. High resolution (60X) images of growth cones from P2 GFP mouse cortical dissociates. (A) Growth cones in three dimensions in collagen gel stained for actin (yellow). In this first image, it appears that the axon also bifurcates before the growth cone and that there are in fact two separate growth cones. (B) Growth cones could also be visualized with GFP in two dimensions on the PLL-coated cover-slip (B). Both methods of imaging yielded high quality images of the growth cone structure. Scale bars 10 μm.

4.0 DISCUSSION

In this study, we successfully designed and built a device to study neurons in low density culture in three dimensions. The purpose of the device is ultimately to monitor and direct differentiation of neural precursor cells into highly specialized populations of motor neurons. To this end, we have successfully optimized culture conditions with mixed cortical cells. Cells were grown in a chamber exposed to media at two ports, and neurite extensions were guided effectively down a 50 μm-wide channel over a length of 500 μm by a gradient of chemoattractant or growth factor.

4.1 Problems, Challenges and Current Experiments

In the course of these experiments, we came across three important challenges: the inhomogeneity of mixed cortical cells, the instability of our chemical gradients, and the inability to take time-lapse images over long periods of time. Perhaps the most important problem we faced was that the mixed cortical cells we used in this study consisted of many different cell types that responded very differently to the same signals. For example, two separate experiments in which bFGF was used as the chemoattractant produced drastically different results (Figures 19 and 20). One "hybrid" cell sent a long axon into the axon channel, but in an identical chip, glial cells were found migrating individually into the axon channel instead. In fact, the chemoattractants we used were really only attractants for growth cones in the traditional sense for a very small subset of cortical cells in the cell suspension. Since the cell culture chamber of the device is so small, it is not guaranteed that a cell capable of responding to the chemoattractant will be present, healthy, and close enough to the axon channel to feel the effects of the gradient and respond accordingly.

This inhomogeneity will continue to be a problem while we use mixed cortical dissociates. In the near future, we hope to use our device on more specialized populations of cells, such as the corticospinal motor neurons. Indeed, the purpose of using cortical dissociates was to optimize culture conditions in the device with a cell that is more readily available and requires less technical preparation. By using a cell type that is more specific and which has a known chemoattractant, we will eliminate much of the variability and chance that contributed to the inconsistencies in our results.

Another important problem we have encountered in these experiments is the sustainability and shape of the chemical gradient. Gradients established by diffusion through fluid are extremely sensitive to mechanical disruptions, and small perturbations of the device such as movement in and out of the incubator, changing the media, or even evaporation from one or more fluid ports can cause micro-scale flows that disrupt the gradient and distort its shape. This phenomenon was extremely apparent in our gradient-testing experiments with FITC-dextran, especially in the additional results reported in Appendix E. The simple movement of the sample on and off of the microscope stage was often enough to disrupt the gradient, and as a result, the experiment had to be repeated several times.

A number of other uncontrolled variable factors may have also contributed to gradient disruption both in these fluorescence experiments and in our cell culture results. When the pressure is not equalized at all ports of the device, small changes in droplet shape and size can result in surface tension forces that generate interstitial fluid flows through the axon channel. In fact, the presence of FITC-dextran (or other chemoattractants or media components) will also alter the surface tension forces exerted by a given droplet, making it even more essential that pressures be controlled across the device. In the experiment shown in Figure E1, for example, small flows likely generated by evaporation of media from the gel-filling channel resulted in a steady gradient over only half of the axon channel; the other half had equilibrated to the concentration of the chemoattractant channel. As a result, growth cones located half-way along the axon channel would not be able to distinguish the gel-filling channel from the axon channel and would likely choose subsequent paths randomly. The cell culture results shown in Figures 17 and 18 are consistent with such a disruption in gradient shape. In this device, axons drifted into the gel-filling channel or, in one case, made an abrupt turn *away* from the chemoattractant channel.

In order to examine the long-term effects of neurons to chemical gradients in the future, we will need to design a device that can maintain a more stable and sustainable gradient. To address this problem, we have already designed and built, but not yet tested, a third version of our system that is compatible with media and chemoattractant flow (Figure 22). PDMS microfluidics chips can be easily connected to a peristaltic pump to control fluid flows through the device. Pressures across the device would need to be

equalized carefully, but introducing flow is advantageous for several reasons. First, a constant flux of fresh media and thorough mixing of the chemoattractant will allow us to create a chemical gradient through the gel that is more sustainable and less sensitive to small perturbations. In addition, the diffusion distance for nutrients to access cells near the axon channel is greatly reduced in this design. Finally, flow past (but not through) the gel actually facilitates diffusive exchange of media into the gel. Furthermore, this design is easier to prepare than our current system.

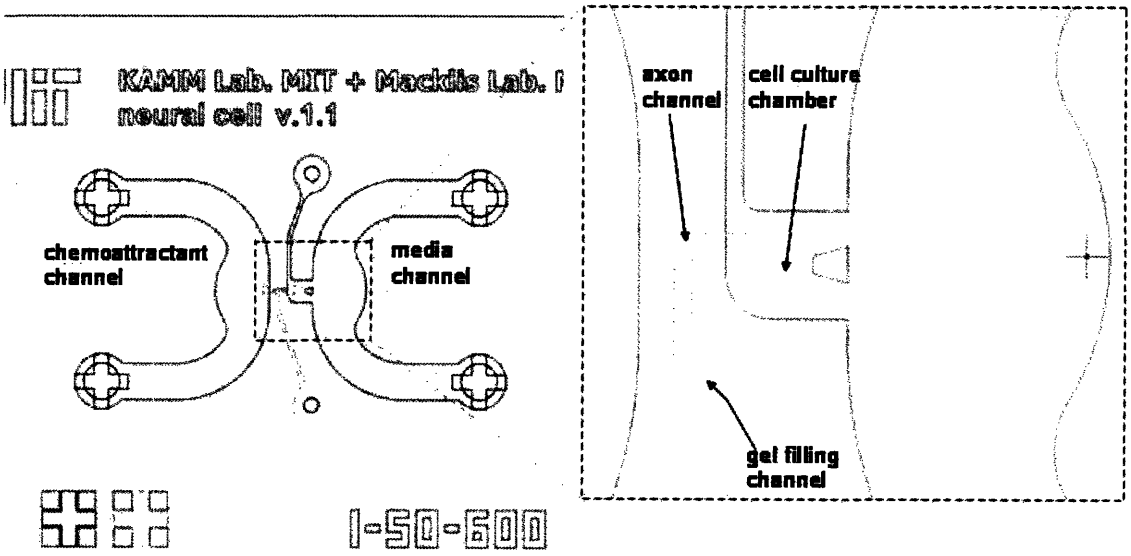

Figure 22. Microfluidic Device for Integration of Flows. Gels will be loaded via the gel filling channel, which will still be 50 μm tall. Cells in a gel suspension will then be loaded through a second channel, 100 μm tall. The PDMS post in the cell culture chamber will stop the flow of gel during loading and provide support for the gel after it has polymerized. (Image courtesy of S. Chung)

Finally, we suspect that some of the inconsistencies in our results are due to sample disruption during imaging. In order to take time-point images, we are currently removing samples from the incubator, and imaging in a microscope room in a separate part of the lab. Moving samples in this manner introduces several potential problems. Neurons are extremely sensitive to small changes in temperature, pH and gas composition. Removing the cells from the incubator for long periods of time is not ideal for their development. In addition, as discussed above, the gradients in the system are very sensitive to small disruptions which can induce transient flows. Moving the samples undoubtedly disrupts the shape of the chemoattractant gradient, potentially resulting in different cellular responses in identical chips.

We are currently working to make our system compatible with continuous imaging on the microscope. Ideally, the chip shown in Figure 22 will be connected to a pump to control chemoattractant and media flow, and kept in a CO_2-perfused, humidified, temperature controlled chamber that can remain on the microscope stage. This continuous *in vitro* imaging will allow us to monitor axon extension and growth cone dynamics in real-time. In addition, we will be able to correlate the cell's response to a developing chemical gradient profile by adding chemoattractant at a known time-point. This capability will be extremely important when determining the specific responses of corticospinal motor neuron precursor cells to developmental growth factors.

4.2 Advantages of Present System

In spite of these problems and challenges, our device still holds several advantages over other microfabricated systems designed for neurons. Perhaps the most important advantage is the ability to examine cell behavior in three dimensions. The gel in the axon channel provides a natural environment for cell survival and neurite outgrowth because the cells are immersed in a three-dimensional scaffold. Previous systems for studying neurons are limited to cell culture on a two-dimensional surface.

The three-dimensional network inside the axon channel also allows direct application of a chemoattractant gradient. Gradients have long been known to be an important factor in growth cone guidance to their targets *in vivo*[38]. There are currently reliable methods for generating controlled gradients in collagen gel[39] or in microfluidic systems[40], but our device integrates the controlled collagen gel gradients into a microfluidic system for three-dimensional directed axon outgrowth.

The design of this device is also favorable for neuron survival. In other systems, cells are grown in small, enclosed channels, reducing the efficiency of gas exchange or waste removal. Because the cell-culture chamber is connected with a large open media well, our system is essentially equivalent to growing neurons in open culture, resulting in healthier cells and more robust axon extension. In addition, when cells must be flowed into a narrow channel, there is an increased risk of damage by shear stress. The chamber in which we grow the cells is several orders of magnitude larger than the cells themselves, greatly increasing their chance of survival while introducing them into the device.

4.3 Future Directions

We plan to use this device as a platform technology to investigate other topics in developmental biology, biomechanics and biomaterials. The device will be extremely useful in a variety of applications because it allows robust cell culture results, and it is possible to vary and control single parameters. Variables could include growth factor or chemoattractant and its concentration, matrix material, or cell type. This level of control over the cell's microenvironment is not otherwise possible using standard cell culture techniques.

4.3.1 Matrix Material Optimization

Although we have not yet done extensive studies in biomaterials with this microfabricated device, we anticipate that it will be useful in optimizing scaffold materials for neural tissue engineering. To this end, we plan to use this culture platform to explore and evaluate matrix materials based on their ability to support neuron survival and axon outgrowth.

Self-assembling peptide hydrogels hold great promise as a scaffold for tissue engineering. Extensive research has already been performed to characterize the aggregation dynamics of ionic self-complimentary oligopeptides which possess an amino acid sequence that leads to self-assembly into β-sheet filaments [e.g., RAD16-I, (RADA)4][41]. These short peptides self-assemble in aqueous salt solution and provide a more natural three-dimensional environment for cell and tissue cultures[42,43,44]. In addition, this scaffold can be functionalized with specific adhesion motifs, conferring the potential for tethering growth factors, chemoattractants or other agents appropriate to our experiments in molecular control[45,46]. Because this peptide was designed as an artificial construct, it is also possible to improve its properties as a scaffold through rational changes in sequence or addition of functional groups. We hope to use the mechanical properties and microarchitecture of this material to guide the improvement of peptide hydrogels for use with engineered tissue implants. We have already successfully grown mouse cortical neurons in this peptide (data not shown), and plan to introduce it into the microfluidic device as a potentially advantageous substitute for collagen.

4.3.2 Growth Cone Dynamics

Our microfluidic culture platform could also provide a simple way to examine the force dynamics between cells and their environments. We have already demonstrated the ability to visualize growth cones with high resolution in the device in both two and three dimensions. Using constitutively fluorescent neurons like the GFP cortical dissociates used in this study, we could also monitor growth cone progress and dynamics of living cells in three dimensions. As a growth cone extends through the channels of our device, it displaces the matrix material (collagen or peptide). By embedding small microbeads within the gel, we can measure these displacements, and obtain more accurate information about the nature of forces exerted by axonal projections. This type of experiment may also reveal interesting subtleties about the projection dynamics of specific populations of neurons, such as the CSMN, compared with other neurons or other motile cell types.

4.3.3 Chemoattractant Studies

We anticipate that in the future we will begin using more complex microfluidic systems with multiple axon channels and/or cell culture chamber designed for specific applications. In addition to our simple single-axon channel design, we are currently building devices with multiple chemoattractant channels, so that we may closely monitor the competing effects of multiple gradients on a small number of cells (Figure 23). Our platform allows us to precisely manipulate the experimental conditions so that multiple chemoattractants and/or chemorepellents could be tested quickly and efficiently on a single group of cells. This level of control is not currently possible using standard cell-culture methods.

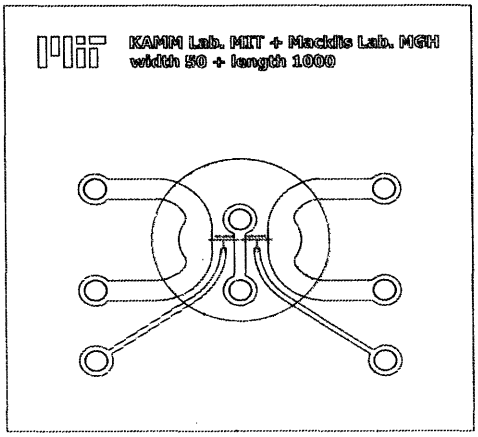

Figure 23. Multi-channel Device. The presence of multiple chemoattractant channels will allow us to examine the effects of competing gradients on neurite direction and outgrowth. (Image courtesy of S. Chung)

4.3.4 Connectivity Studies

Another goal of devices with multiple axon channels and cell chambers is to closely monitor and investigate the connectivity of specific populations of neurons (such as the CSMN) (Figure 24). This platform will allow us to locate neurons in each cell culture chamber and direct axonal outgrowth with a chemoattractant gradient in one direction. An additional benefit of this design is that we can seed different populations of neurons in each channel as a way of recapitulating neuronal circuits within the device. For example, CSMN could be cultured in one chamber and form connections with lower motor neurons, which could in turn form connections with muscle cells in a third compartment. This level of control over axonal connections between specific cell types is not currently possible using standard cell-culture methods. Being able to understand and control the projection and connectivity of neurons like the CSMN would be a significant step towards therapeutic regeneration of cells after damage or disease.

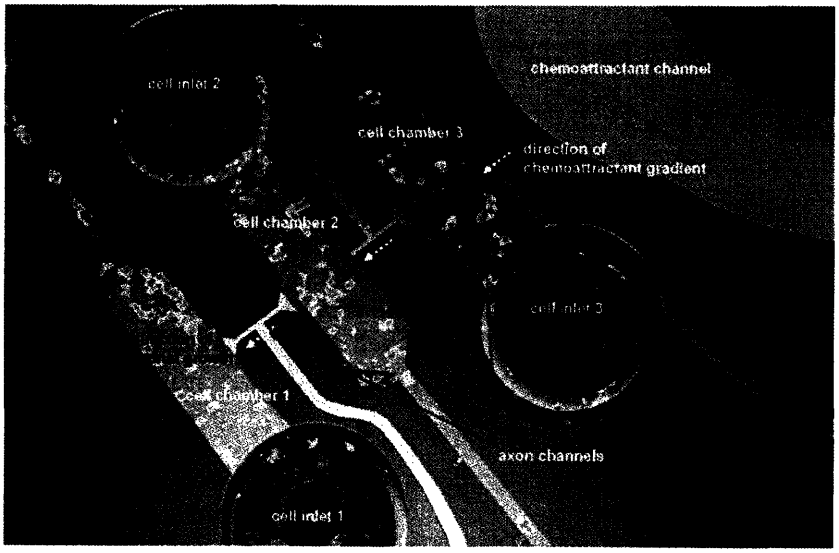

Figure 24. Microfluidic Device for Connectivity Studies. This device has multiple cell chambers and axon channels to facilitate cell-cell connections. Neurons will be cultured in each cell chamber in a gel containing different concentrations of chemoattractant. Gels will be filled through gel-filling inlets (not shown) as in previous designs. The chemical gradient will therefore extend through all three cell chambers, directing axons to extend only in the direction of the chemoattractant gradient. In this way, we can guide connections between different cell populations. (Image courtesy of S. Chung).

4.3.5 Vertical Bioreactor for Neurons

A different microfluidic system, the vertical bioreactor, contains multiple axon channels and allows high-throughput experimentation by generation of a vertical gradient of chemoattractant through gel (Figure 25). This system would allow us to grow many neurons in each chip, each in its own axon channel. In addition, this system could eventually be adapted for implantation by using a biodegradable, biocompatible polymer instead of PDMS, and directing growth of a specific population of neurons into the body. This type of device might even eventually enable regeneration or repair of damaged motor output circuitry after damage sustained by ALS or other neurodegenerative diseases.

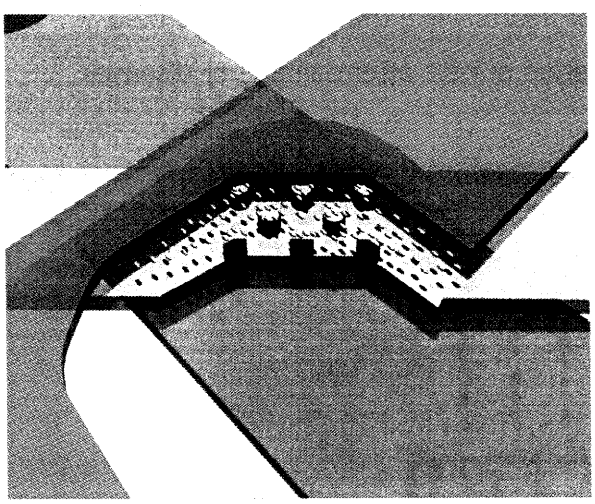

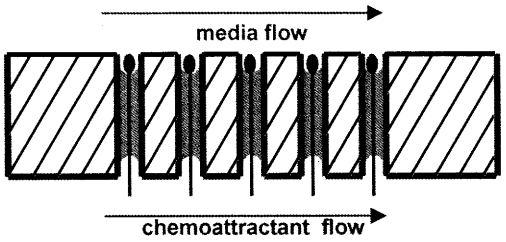

Figure 25. Vertical Bioreactor for Neuron Culture. Neurons will be cultured in individual channels filled with collagen gel. Culture media will be flowed over the top of the cells and chemoattractant flowed below the cells. A gradient of chemoattractant will be established through the gel. (Images courtesy of S. Chung.)

4.4 Concluding Remarks

Research with this device occupies a unique position at the interface of developmental cell biology, neuroscience, advanced biomaterials and microfluidics technology. Microfabricated cell-culture systems will enable us to investigate the molecular and cellular controls over a highly specialized population of neurons, and osur results may help elucidate the basic developmental biology of CSMN. Future studies investigating these critical neurons may result in the ability to regenerate corticospinal circuitry from endogenous neural stem cells after brain damage. This achievement would represent a groundbreaking advancement in therapeutic options for many common neurodegenerative diseases.

REFERENCES

[1] Gordon-Weeks PR. (2000) Neuronal growth cones. Cambridge: Cambridge University Press.

[2] Guan KL, Rao Y (2003) Signalling mechanisms mediating neuronal responses to guidance cues. *Nature Rev Neurosci* 4: 941–956.

[3] Rehder V, Kater SB. (1996) Filopodia on neuronal growth cones: Multifunctional structures with sensory and motor capabilities. *Seminars in the Neurosciences* 8: 81–88.

[4] Winhammar JM, Rowe DB, Henderson RD, Kiernan MC. (2005). Assessment of disease progression in motor neuron disease. *Lancet Neurol* 4: 229-238.

[5] Kandel ER Schwartz JH, Jessel TM. (1991) Principles of Neural Science. 3rd edition. East Norwalk: Appleton & Lange.

[6] Goodall EF, Morrison KE. (2006) Amyotrophic lateral sclerosis(motor neuron disease): proposed mechanisms and pathways to treatment. Expert Reviews in Molecular Medicine 8(11): 1-22.

[7] Mulder DW et al. (1986) Familial adult motor neuron disease: amyotrophic lateral sclerosis. *Neurology* 36(4): 511-517

[8] Bruijn LI, Cudkowicz M. (2006) Therapeutic targets for amyotrophic lateral sclerosis: current treatments and prospects for more effective therapies. *Expert Rev Neurother* 6(3): 417-28.

[9] ALS Association. "Facts You Should Know About ALS." http://www.alsa.org/als/facts.cfm?CFID=2628852&CFTOKEN=25592082

[10] Bruijn LI, Miller TM, Cleveland DW. (2004) Unraveling the mechanisms involved in motor neuron degeneration in ALS. *Annu Rev Neurosci* 27: 723-749.

[11] Pasinelli P, Brown RH. (2006) Molecular biology of amyotrophic lateral sclerosis: insights from genetics. *Nat Rev Neurosci* 7: 710-723.

[12] Weiss S, Dunne C, Hewson J, Wohl C, Wheatley M, Peterson AC, Reynolds BA. (1996) Multipotent CNS stem cells are present in the adult mammalian spinal cord and ventricular neurotaxis. *J Neurosci* 16: 7599-7609.

[13] Dunnett SB, Bjorklund A (2000) Functional transplantation II: novel cell therapies for CNS disorders. In: Progress in brain research, Vol 127 (Dunnett SB, Bjorklund A, eds), pp 1-559. Oxford: Elsevier Science.

[14] Fricker-Gates RA, Shin JJ, Tai CC, Catapano LA, Macklis JD. (2002) Late-Stage Immature Neocortical Neuron Reconstruct Interhemispheric Connections and Form Synaptic Contacts with Increased Efficiency in Adult Mouse Cortex Undergoing Targeted Neurdegeneration. *J Neurosci* 22(10): 4045-4056.

[15] Chen J, Magavi SSP, Macklis JD. (2004) Neurogenesis of corticospinal motor neurons extending spinal projections in adult mice. *Proc Nat Acad Sci* 101(46): 16357-16362.

[16] Arlotta P, Molyneaux B, Chen J, Inoue J, Kominami R, Macklis JD. (2005) Neuronal Subtype-Specific Genes that Control Corticospinal Motor Neuron Development In Vivo. *Neuron* 45: 207-221.

[17] Molyneaux BJ, Arlotta P, Hirata T, Hibi M, Macklis JD. (2005) Fezl Is Required for the Birth and Specification of Corticospinal Motor Neurons. *Neuron* 47: 817-831.

[18] Ozdinler PH, Macklis JD. (2006) IGF-1 specifically enhances axon outgrowth of corticospinal motor neurons. *Nat Neurosci* 9(11): 1371-1381.

[19] Giehl KM. (2001). Trophic dependencies of rodent corticospinal neurons. *Rev Neurosci.* 12: 79-94.

[20] Voldman J, Gray ML, Schmidt MA. (1999) Microfabrication in biology and medicine. *Annu Rev Biomed Eng* 1:401-25.
[21] Whitesides GM, Ostuni E, Shuichi T, Jiang X, Ingber DE. (2001) Soft Lithography in Biology and Biochemistry. *Annu Rev Biomed Eng* 3: 335-73.
[22] Tourovskaia A, Rodriguez-Zas X, Folch A. (2005) Long-term micropatterned cell cultures in heterogeneous microfluidic environments. *Lab Chip*, 5(1): 14–19.
[23] McDonald JC, Whitesides GM. (2002) Poly(dimethylsiloxane) as a material for fabricating microfluidic devices. *Acc Chem Res* 35(7): 491-99.
[24] Taylor A, Blurton-Jones M, Rhee SW, Cribbs DH, Cotman CW, Jeon NL. (2005) A microfluidic culture platform for CNS axonal injury, regeneration and transport. *Nature Methods* 2(8): 599-605.
[25] Chung BG, Flanagan LA, Rhee SW, Schwartz PH, Lee AP, Monuki ES, Jeon NL. (2004) Human neural stem cell growth and differentiation in a gradient-generating microfluidic device. *Lab Chip* 5: 401-406.
[26] Song H, Poo MM. (2001). The cell biology of neuronal navigation. *Nat Cell Biol*, 3: E81–88.
[27] Patolsky F, Timko BP, Yu G, Fang Y, Greytak AB, Zheng G, Lieber CM. (2006) Detection, stimulation and inhibition of neuronal signals with high-density nanowire transistor arrays. *Science* 313(5790): 1100-4.
[28] Cukierman E, Pankov R, Yamada KM. (2002) Cell interactions with three-dimensional matrices. *Curr Opin Cell Biol* 4(5): 633-9.
[29] Goslin G, Banker K. (1998) Culturing Nerve Cells, 2nd ed. Cambridge: MIT Press.
[30] Lodish H, Berk A, Zipursky LS, Mastudaira P, Baltimore D, Darnell J. (2000) Molecular Cell Biology, 4th ed. New York: WH Freeman and Co.
[31] Tranquillo RT. (1999) Self-Organization of Tissue-Equivalents: The Nature and Role of Contact Guidance. *Biochemical Society Symposia*, 65: 27–42.
[32] Roeder BA, Kokini K, Surgis JE, Robinson JP, Voytik-Harbin SL. (2002) Tensile Mechanical Properties of Three-Dimensional Type I Collagen Extracellular Matrices with Varied Microstructure. *J Biomech Eng*, 124: 214–223.
[33] Nauman JV, Campbell PG, Lanni F, Anderson JL. (2007) Diffusion of Insulin-like Growth Factor-1 and Ribonuclease through Fibrin Gels. *Biophys J*. Published ahead of print as doi:10.1529/biophysj.106.102699.
[34] Thiagarajah JR, Pedley KC, Naftalin RJ. (2001) Evidence of amiloride-sensitive fluid absorption in rat descending colonic crypts from fluorescence recovery of FITC-labeled dextran after photobleaching. *J Phisiol,* 536(2): 541-553.
[35] Gribbon P, Hardingham TE. (1998) Macromolecular Diffusion of Biological Polymers Measured by Confocal Fluorescence Recovery after Photobleaching. *Biophys J*, 75(2): 1032-1039.
[36] Holland EC, Varmus HE. (1998) Basic fibroblast growth factor induces cell migration and proliferation after glia-specific gene transfer in mice. *Proc Natl Acad Sci*, 95(3): 1218-1223.
[37] Le R, Esquenazi S. (2002) Astrocytes mediate cerebral cortical neuronal axon and dendrite growth, in part, by release of fibroblast growth factor. *Neurol Res*, 24(1): 81-92.
[38] Baier H, Bonhoeffer F. (1992) Axon guidance by gradients of a target-derived component. *Science* 255: 472–475.
[39] Rosoff WJ, McAllister R, Esrick MA, Goodhill GJ, Urbach JS. (2005) Generating controlled molecular gradients in 3D gels. *Biotechnol Bioeng* 91(6): 754-9.

[40] Saadi W, Wang SJ, Lin F, Jeon NL. (2006) A parallel-gradient microfluidic chamber for quantitative analysis of breast cancer cell chemotaxis. *Biomed Microdevices* 8: 109-118.
[41] Hwang W, Zhang S, Kamm RD, and Karplus M. Kinetic control of dimer structure formation in amyloid fibrillogenesis. *Proc Natl Acad Sci* 101: 12916-12921, 2004.
[42] Narmoneva DA, Oni O, Sieminski AL, Zhang S, Gertler JP, Kamm RD, Lee RT. (2005) Self-assembling short oligopeptides and the promotion of angiogenesis. *Biomaterials* 26(23):4837-46.
[43] Sieminski, Was, Kim and Kamm, in revision for *Cell Biochemistry and Biophysics*.
[44] Narmoneva DA, Vukmirovic R, Davis ME, Kamm RD, Lee RT. Endothelial cells promote cardiac myocyte survival and spatial reorganization: Implications for cardiac regeneration. *Circulation*, 110:962-968, 2004.
[45] Genove E, Shen C, Zhang S, Semino CE. (2005) The effect of functionalized self-assembling peptide scaffolds on human aortic endothelial cell function. *Biomaterials* 26(16):3341-51.
[46] Davis ME, Motion JP, Narmoneva DA, Takahashi T, Hakuno D, Kamm RD, Zhang S, Lee RT. (2005) Injectable self-assembling peptide nanofibers create intramyocardial microenvironments for endothelial cells. *Circulation* 111(4):442-50.
[47] Sanjana NE, Fuller SB. (2004) A fast flexible ink-jet printing method for patterning dissociated cells in culture. *J Neurosci Meth* 136(2):151-163

Appendix A. Comparison of Sources of Neural Tissue

	Rat Cortical Cells	GFP Mouse Cortical Cells
Source	Massachusetts Institute of Technology Dep't of Brain and Cognitive Science Howard Hughes Medical Institute Sebastian Seung Lab	Massachusetts General Hospital/ Harvard Medical School Center for Nervous System Repair Jeffrey Macklis Lab
Stage of animal	Postnatal day 0 – 1	Postnatal day 0 – 2
Advantages of cell source	- Longer life span in the devices (over 7-10 days) - Large and frequent supply of cells - Tissue can be kept overnight in cold culture medium and used up to 24 hours after dissection with reasonable cell viability - Cells are readily available and easily acquired (across the street)	- GFP reporter available for *in vivo* fluorescence imaging - Glial cells do not migrate into channels - Glial cells take longer to proliferate and become confluent
Disadvantages of cell source	- Extremely aggressive glial cells will migrate and proliferate within a few days - Long axons do not appear for 3-4 days (after massive glial proliferation) - Absence of GFP or other fluorescent reporter – rely on phase contrast imaging for *in vivo* imaging	- Cells and axons tend to die and retract after 3-4 days in the devices - Less readily available tissue source - Cells must be transported from MGH

Images
4 days *in vitro*
(scale bar: 100 µm)

Rat cortical Cells

GFP Mouse Cortical Cells

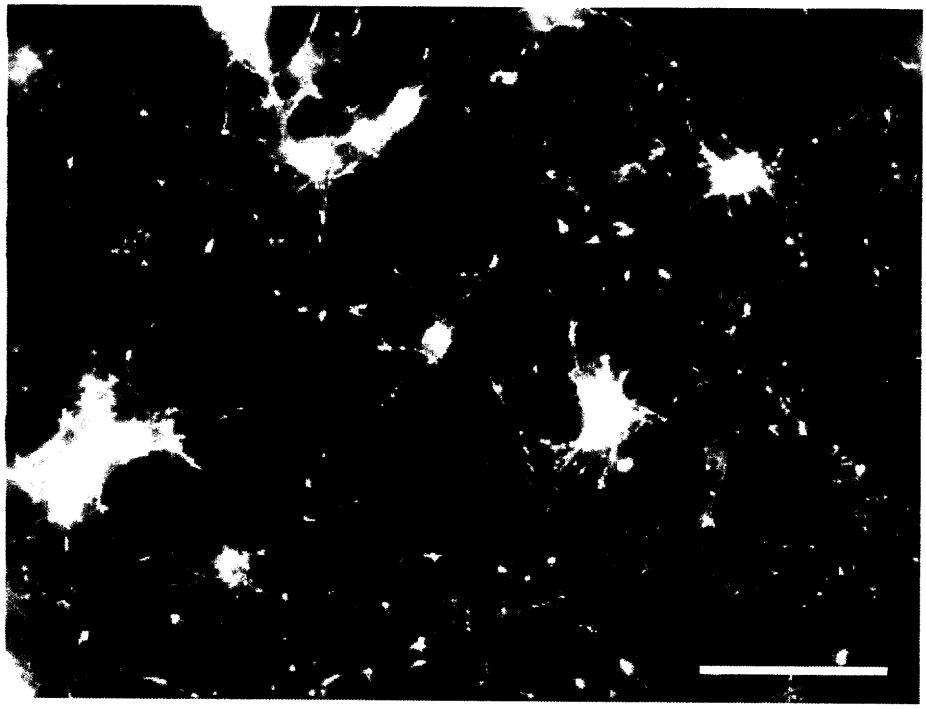

Appendix B. Dissociation and Cell Culture Protocol[1]

1. SOLUTIONS (prepared fresh before each dissociation)

Dissociation Media (DM)[2] -- pH to 7.35, filter, keep on ice
40 mL ddH_2O
5 mL 10X DM (prepared by Macklis lab at MGH)[3]
5 mL Mg/Kynurenate (prepared by Macklis lab at MGH)
600 µL 20 mM Glucose (Sigma)
500 µL 5 mM AP5 (D(-)-2-amino-5-phosphonovaleric acid (Sigma), a selective NMDA receptor antagonist)
500 µL Penicillin/Streptomycin (P/S, Sigma)

Enzyme Solution -- pH to 7.35, filter, warm to 37°C before dissociation
10 mL DM (the complete solution described above)
1.6 mg cysteine (100 µL of 16 mg/mL stock, prepared in ddH_2O)
100 units of Papain (Worthington)
Add 50 µL DNAse stock after filtration (0.2 mg/mL, prepared in filtered ddH_2O)[4]

Inhibitor Solution -- pH to 7.35, filter, keep on ice
5.4 mL DM
600 µL Ovomucoid/Bovine Serum Albumin[5] (prepared by Macklis lab at MGH)

OptiMEM Trituration Solution -- pH to 7.35, filter, keep on ice
50 mL OptiMEM (Gibco)
2.5 mL Mg/Kynurenate
600 µL 30% Glucose
250 µL AP5

Serum Containing Media (SCM) -- pH to 7.35, filter, keep on ice[6]
42.5 mL Neurobasal A Medium (NBA, Gibco)
5 mL Fetal Bovine Serum (FBS, Hyclone)
0.5 mL 3.75 M NaCl (dissolved in NBA)
0.5 mL 30% Glucose
0.5 mL B27 Supplement (Gibco)
0.5 mL P/S
0.5 mL L-Glutamine (100X)

---

[1] This protocol has been adapted from dissociation protocols from the Jeffrey Macklis lab at Mass General Hospital (MGH)[18] and the Sebastian Seung lab at the MIT department of Brain and Cognitive Science.[47]
[2] If reagents for DM are unavailable, HBSS supplemented with 2.38 g/L HEPES may also be used.
[3] Ingredients for these solutions will be presented in section 3 of the appendix
[4] DNase is subject to shear-induced denaturation, and should be added to the enzyme solution after filtration through a 0.2 µm-syringe filter.
[5] If Ovo/BSA stock is unavailable, inhibitor solution can be prepared from 5 mL DM and 5 mL serum. While it does not contain Trypsin inhibitors, serum is effective at quenching the protease reaction.
[6] Media should be warmed to 37°C before it is added to cells

2. CORTICAL DISSOCIATION PROCEDURES

1. Keep cortices on ice in DM in a small petri plate. Cut tissue into small pieces. This increases the surface area over which the enzymatic digestion can act.
2. Transfer tissue to a 15 mL falcon tube using a high-aperture transfer pipette.
3. Rinse cortices 2-3 times with 10 mL DM. Allow the tissue to settle after each wash and then aspirate the supernatant.
4. Carefully remove any remaining DM, and add 5 mL of warm enzyme solution. Tilt the falcon tube in order to maximize contact area between the tissue pieces and the enzyme. Keep at 37°C.
5. After 5-7 minutes, remove as much enzyme as possible without disturbing cortices, and add 5 mL of fresh warm enzyme solution.
6. After 5-7 minutes, remove remaining enzyme. Cortices can become stuck together by DNA from lysed cells at this stage, so enzyme removal must be done very carefully.
7. Add inhibitor solution to tissue and let sit for 1-2 minutes at room temperature.
8. Rinse cortices 2-3 times in 5-10 mL OptiMEM solution to remove all enzyme and inhibitor.
9. Add 1 mL OptiMEM solution to cortices, and mechanically dissociate through a white 1 mL pipette tip. Pipette very slowly and gently 6-8 times. This is very important, as over-dissociating can easily damage the delicate postnatal neurons. Keep cells and solutions cold.
10. Allow tissue chunks to settle while the falcon tube is kept in ice. Remove the supernatant to a new falcon tube. This contains the single-cell suspension.
11. Add another 1 mL OptiMEM to the tissue chunks and continue triturating. Repeat pipette-settle-remove supernatant cycle until all tissue is dissociated or until the desired number of cells is attained.
12. In order to separate cellular debris and membranes from live cells, centrifuge cell suspension at 800-1200 rpm for 4 minutes. Resuspend pellet in cold SCM by tapping the falcon tube rather than with a pipette. The cells are now ready to be plated in collagen, on PLL or in PDMS devices, but keep cells on ice until they are put in culture.
13. Culturing cells on PLL: Dilute cells to appropriate density (~10^5 cells/ml) in warm SCM and plate on PLL-coated culture plates or cover-slips.
14. Culturing cells in collagen: add cells to a concentrated collagen pre-gel solution prepared in CM[7] and adjusted to pH 7.35. Allow collagen to polymerize for 10 minutes before adding media on top.

    (Using BD Biosciences Rat Tail Type I Collagen, 3.56 mg/ml in acetic acid):

0.35 mg/ml collagen	0.5 mg/ml collagen	2.0 mg/ml collagen
20 µL collagen	28.5 µL collagen	114.3 µL collagen
140 µL CM	112.5 µL CM	45.7 µL CM
40 µL cell suspension	40 µL cell suspension	40 µL cell suspension

15. Culturing cells in PDMS devices: Flow 4-5 µL of cell suspension (in media or collagen) into the cell culture chamber. Keep in incubator for 5-10 min to allow collagen polymerization or cell adhesion before adding media to media well.

[7] CM: Conditioned Media. Made by conditioning SCM on cultures of P0 neurons overnight.

3. SOLUTIONS PREPARED AT MGH

10X DM Stock
0.55 g $MgCl_2$
4.0 ml 14 mM (0.5%) Phenol Red
1.6 ml Hepes (1M)
2 ml NaOH (0.1 N)
12.78g Na_2SO_4
5.23 g K_2SO_4
H_2O to 100 mL
** Filter and store at room temperature

Mg/Kynurenate Stock
95 mL H_2O
151.4 mg Kynurenic acid
400 µL Phenol red
** pH to 7.35, then add the rest of the ingredients
400 µL HEPES
0.76 g $MgCl_2$
H_2O to 100 mL
** Filter, aliquot to 7.5 mL and store at -20°C

Ovomucoid/BSA
100 mg/ml ovomucoid
100 mg/ml BSA
** Filter, aliquot 600 µl and store at -80°C

Appendix C. Two-Level Photolithography Protocol

The following procedure was adapted by Sid Chung from protocols recommended by MicroChem Corporation on their website:
http://www.microchem.com/products/pdf/SU-82000DataSheet2025thru2075Ver4.pdf

Level 1: Axon and Gel-Filling Channel

1) **Dehydration**: Keep wafer at 200°C for 10 minutes to completely dehydrate
2) **Spin-Coat**: SU-8 2050
   - Dispense photoresist onto wafer
   - Spin at 500 rpm for 10 seconds
   - Spin at 3000 rpm for 30 seconds
3) **Soft Bake** (on a hot-plate)
   - 65°C for 2 minutes
   - 95°C for 8 minutes
4) **Interval Exposure**: expose coated wafer to UV light through the transparency mask for five intervals of exposure followed by rest to prevent burn-out. No alignment is necessary for the first transparency.
5) **Post Exposure Bake** (on a hot-plate)
   - 65°C for 1 minute
   - 95°C for 5 minutes
6) **Development**: Develop in PM Acetate solution followed by Isopropyl Alcohol (IPA) rinse. Dry wafer thoroughly with filtered, pressurized nitrogen.

Level 2: Chemoattractant Channel and Cell Culture Chambers

** Skip Dehydration step, which might damage SU-8 patterns already on the wafer
1) **Spin-Coat**: SU-8 2050
   - Dispense photoresist onto wafer
   - Spin at 500 rpm for 10 seconds
   - Spin at 1500 rpm for 30 seconds
2) **Soft Bake** (on a hot-plate)
   - 65°C for 6 minutes
   - 95°C for 25 minutes
3) **Interval Exposure**: expose coated wafer to UV light through the transparency mask for five intervals of exposure followed by rest to prevent burn-out. Use alignment grid found on both transparencies to make sure channels are properly oriented.
4) **Post Exposure Bake** (on a hot-plate)
   - 65°C for 4 minute
   - 95°C for 15 minutes
5) **Development**: Develop in PM Acetate solution followed by Isopropyl Alcohol (IPA) rinse. Dry wafer thoroughly with filtered, pressurized nitrogen.

Appendix D. Staining and Imaging Procedures

Cell Fixation

1) Gently remove media from media well.
2) Add 200-300 µL 4% Paraformaldehyde (PFA) to the media well of each sample, and allow fixation for approximately 25 minutes.
3) Remove PFA to appropriate waste container, and wash with 300 µL PBS for 10 minutes.
4) Repeat PBS wash.
5) Wash with 200 µL 0.1% Triton-X for 1-2 minutes.
6) Wash twice with PBS.

Staining

1) Prepare stain in the following ratio:
   1 mL PBS
   4 µL DAPI (1000x) (labels nucleus)
   12.5 µL Rhodamine-Phalloidin (labels actin)
2) Add 100 µL of stain to each media well and cover samples with aluminum foil (to preserve the fluorophores) for at least 30 minutes.
3) Wash twice with PBS for 10 minutes.

Imaging Tips

1) Clean bottom of chip with ethanol to remove any residues of media, PBS, or fingerprints. Dry well and place chip alone on microscope stage (not in plastic).
2) Keep PBS interface even across the top of the media well. If the curvature of the droplet is too high, light will be refracted, and it will be difficult to focus on small structures.
3) GFP photobleaches quickly when the fluorescence light is at high intensity. Do not expose GFP samples to unnecessary fluorescence.

Appendix E. Additional Resources for Gradient Testing

1. MATLAB Code for Gradient Quantification

Assumptions: Fixed concentration at the ends of the gel region

Run m-file multiple times for each data set (changing the gradient image file and the color of the line on the plot)

gradient.m

```
clear all
hold on

%import gradient image tif file
img = imread('C:\MATLAB72\work\1.tif');

%convert image uint16 file to double
double = double(img);

%take average value at each x-value along the gradient
avg = mean(double,1);

%define concentration at cell culture chamber
zero = min(avg);

%define concentration at chemoattractant channel
max_conc_A = max(avg);

%subtract zero-concentration value from each pixel value, and max_conc
avg_shift = avg-zero;
max_conc = max_conc_A-zero;

%normalize to concentration in chemoattractant channel
avg_norm = avg_shift./max_conc;
%avg_norm = avg./max_conc_A;

%convert fraction values to concentration in uM
avg_eq = avg_norm.*10;

%define parameters for plotting
length = max(size(avg_eq));
step = (length-1);

%define X-axis in um along 600 um channel
x = (0:600/step:600);

%plot concentration gradient as a function of x-distance along channel
plot(x,avg_eq, 'r')
```

2. Results of Additional Gradient-Testing Experiments

For a number of gradient testing experiments, we used devices without the small hole shown in Figure 13 for ease of imaging. We also neglected to control the humidity of the devices throughout the experiment. Fluorescence images were taken every 30 minutes for 5 hours and again at 10 hours. The developing gradient profile can be seen in Figure E1 below.

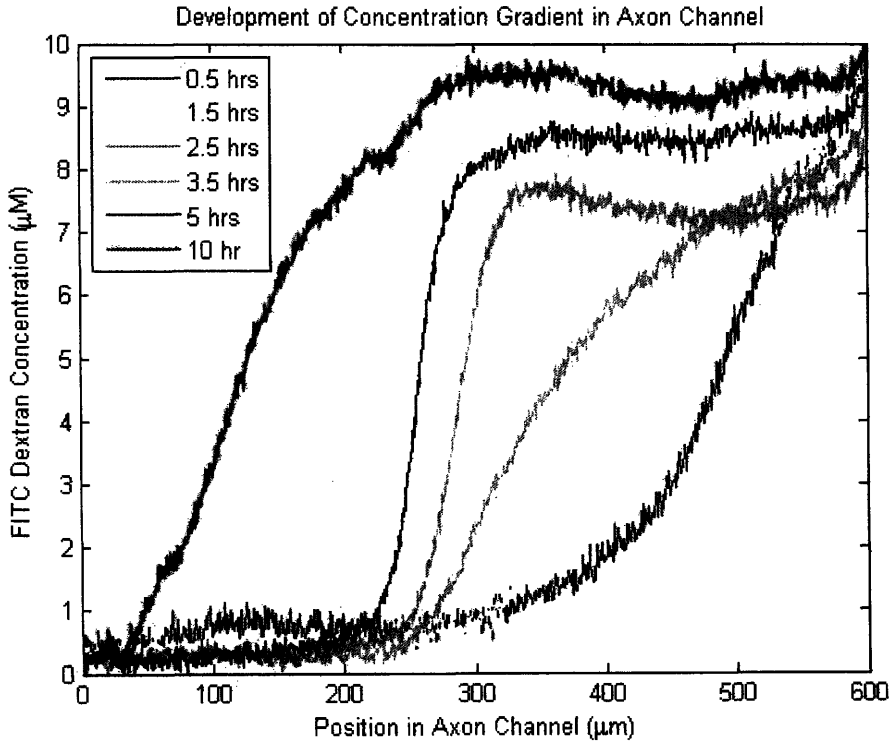

Figure E1. Development of a Concentration Gradient of Chemoattractant in the Axon Channel. FITC- dextran (10 kDa, 10 μM) was used as a tracer to monitor diffusion through the axon channel. The concentration at the cell culture chamber was held at zero.

At time points prior to 1.5 hours, the concentration profile appears to rise towards the expected linear gradient across the axon channel; however, after 2 hours, the concentration of tracer begins rising much faster in the right side of the axon channel (region 1 in Figure E2) than in the left (region 2). By 3.5 hours, the concentration of tracer appears to have leveled-off on the left side of the channel, at which point a linear gradient begins to develop in the right side of the axon channel.

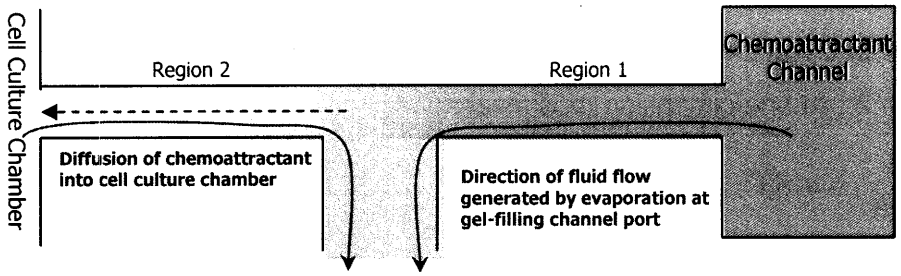

Figure E2. Schematic of transport in the axon channel. In the data pictured in the previous figure, transport occurs by diffusion from the chemoattractant channel and convection into the gel-filling channel. Convective processes are likely generated by a slight pressure gradient arising from evaporation of liquid at the gel-filling port.

Mass transport by diffusion is dependent upon the presence of a concentration gradient, as expressed by Fick's first law, which states that:

$$J = -D\frac{\partial C}{\partial x}$$

where J is the mass flux per unit area due to diffusion, C is the concentration of the molecule of interest and D is the diffusion coefficient. Gradient profiles at early time points (until 1.5 hours) are consistent with diffusion-dominated transport of tracer through the axon channel; however by 3.5 hours, there appears to be no gradient at all in region 1 of the device. In the absence of a concentration gradient, a small convective flow through region 1 of the axon channel must have been present to account for the transport of tracer into the axon channel.

The concentration profiles at 2.5 and 3.5 hours suggest that a slight pressure drop developed in the gel-filling channel, likely from evaporation at the gel-filling port. Evaporation had been previously observed in these devices, which lack a hole in the gel-filling channel to equalize pressures across the axon channel. The 10 hour time-point, on the other hand, is somewhat contradictory. The even linear gradient in region 2 is strongly suggestive of a diffusion-dominated process with little to no convective flow; however the lack of gradient in region 1 requires that flow was present in order to account for transport of chemoattractant into region 2.

Although it is difficult to say exactly what processes are at work in this 10 hour time-point, we can use it to make some estimates about the limits for the flow velocity. We first ignore the gel-filling channel, and assume that transport in region 1 is convection-dominated, but transport in region 2 is diffusion-dominated. We can then

extrapolate a lower-limit value for the flow rate by noting that at steady state, the convective flux of tracer through region 1 must be equal to the diffusive flux of tracer through region 2. In one dimension, this means:

$$DA_2 \frac{dC_2}{dx} = u_1 A_1 C_1$$

The cross-sectional areas $A_1 = A_2 = 2500\ \mu m^2$, and D is the diffusivity of the FITC-dextran. C_1 is the steady concentration in region 1 and dC_2/dx is the slope of the concentration gradient in region 2. From this equation and the values taken from Figure E1, we calculate u_1, the velocity of liquid moving through the channel, to be 1.8 μm min^{-1}. This value must be a lower-limit for the actual fluid velocity in the axon channel, since in the real device, a substantial amount of chemoattractant would be traveling up the gel-filling channel, and the velocity in region 1 must be higher to provide an adequate flux of tracer to account for the gradient observed in region 2.

A pressure gradient driving flow up the gel-filling channel was previously observed in these devices when evaporation occurred at the gel-filling port. Evaporation in a humidified chamber from a tube with a diameter of 4 mm was observed at approximately 20 μL day^{-1}. When normalized to the cross-sectional area of the container, this value corresponds to a flow velocity of approximately 1 μm min^{-1}. Although this value is slightly lower than the flow-rate observed for this experiment, it is important to note that these numbers for evaporation were obtained in a humidified chamber, where evaporation takes place much more slowly.

The results of this experiment primarily indicate a need to monitor the gradient (and confounding factors that might disrupt it) much more carefully. Differential evaporation, fluid pressures, and solute concentrations are all variables that must be carefully examined before and during an experiment. Although we have shown in section 3.4 that we can minimize the effects of evaporation on the chemical gradient by using updated devices in a humidified chamber, these and other extraneous variables can still have profound effects on the gradient size and shape. These variables likely played an important role in the discrepancies observed in our cell culture results.